DIS '96
[ROMA]

INCLUSIVE MEASUREMENTS OF DIFFRACTION THROUGHOUT THE HERA Q^2 RANGE

Paul Newman
University of Birmingham
For the H1 Collaboration

- Mass Distribution, $\frac{d\sigma}{dM_X^2}$ in Diffractive Photoproduction.
- Total Diffractive Cross-Sections in Photoproduction.
- The Diffractive Structure Function, $F_2^{D(3)}(Q^2, \beta, x_{I\!P})$.
- Factorisation Tests.
- Partonic Structure of the Diffractive Exchange.

DIFFRACTIVE PROCESSES IN PHOTOPRODUCTION

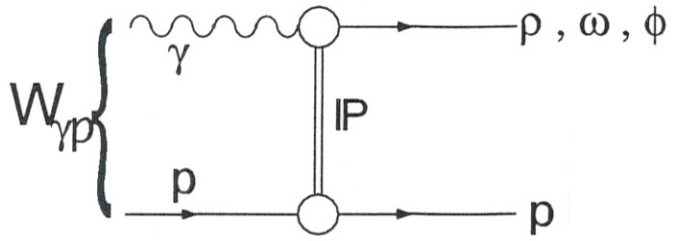

QUASI ELASTIC VECTOR MESON PRODUCTION

(EL)

$\gamma p \longrightarrow Vp$

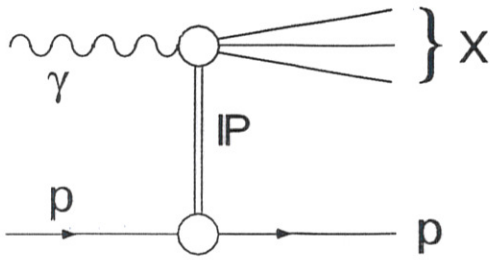

SINGLE PHOTON DISSOCIATION

(GD)

$\gamma p \longrightarrow Xp$

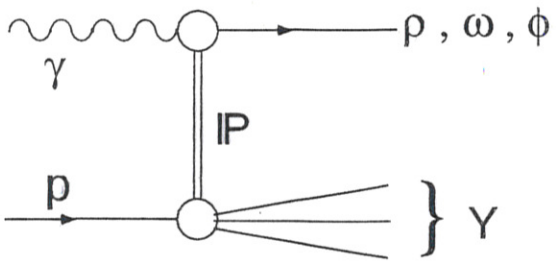

SINGLE PROTON DISSOCIATION

(PD)

$\gamma p \longrightarrow VY$

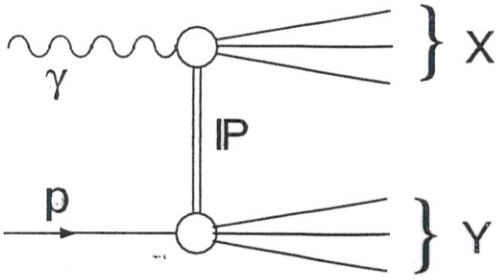

DOUBLE DISSOCIATION

(DD)

$\gamma p \longrightarrow XY$

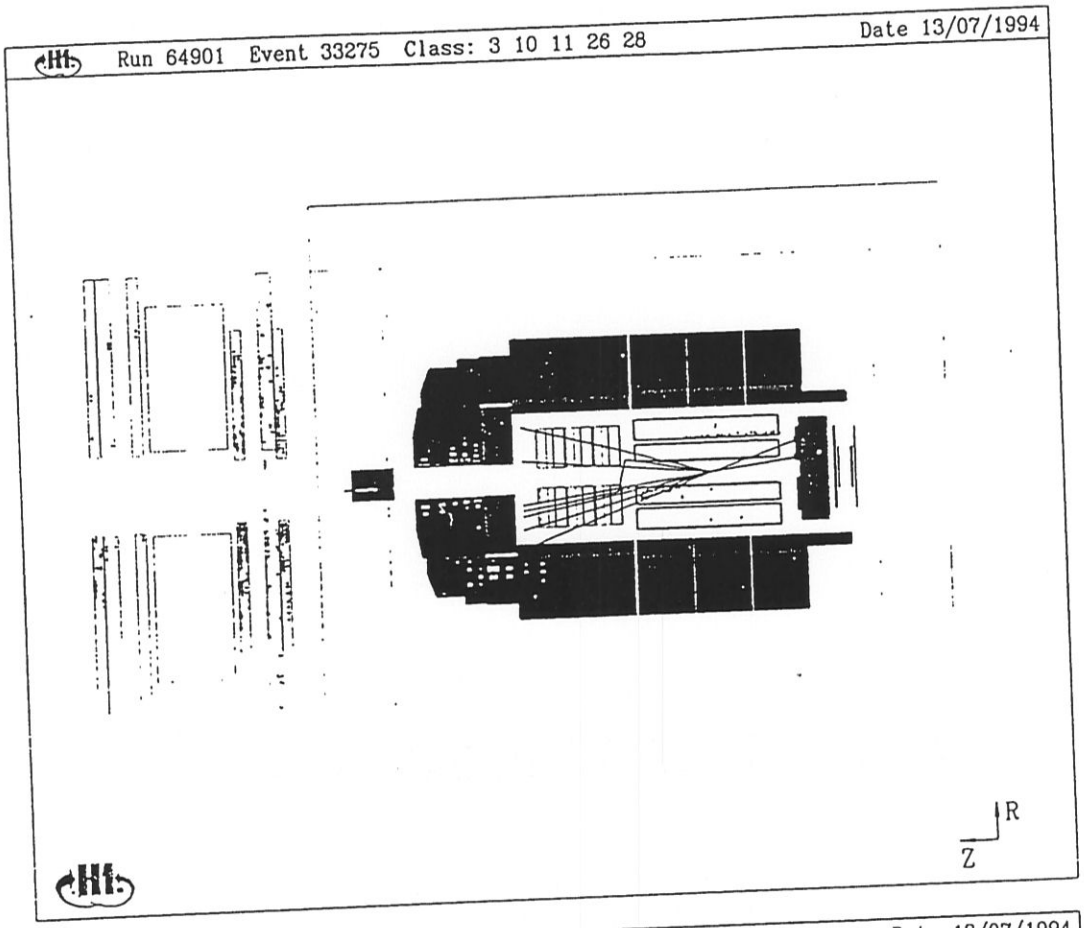
Run 64901 Event 33275 Class: 3 10 11 26 28
Date 13/07/1994
R
Z

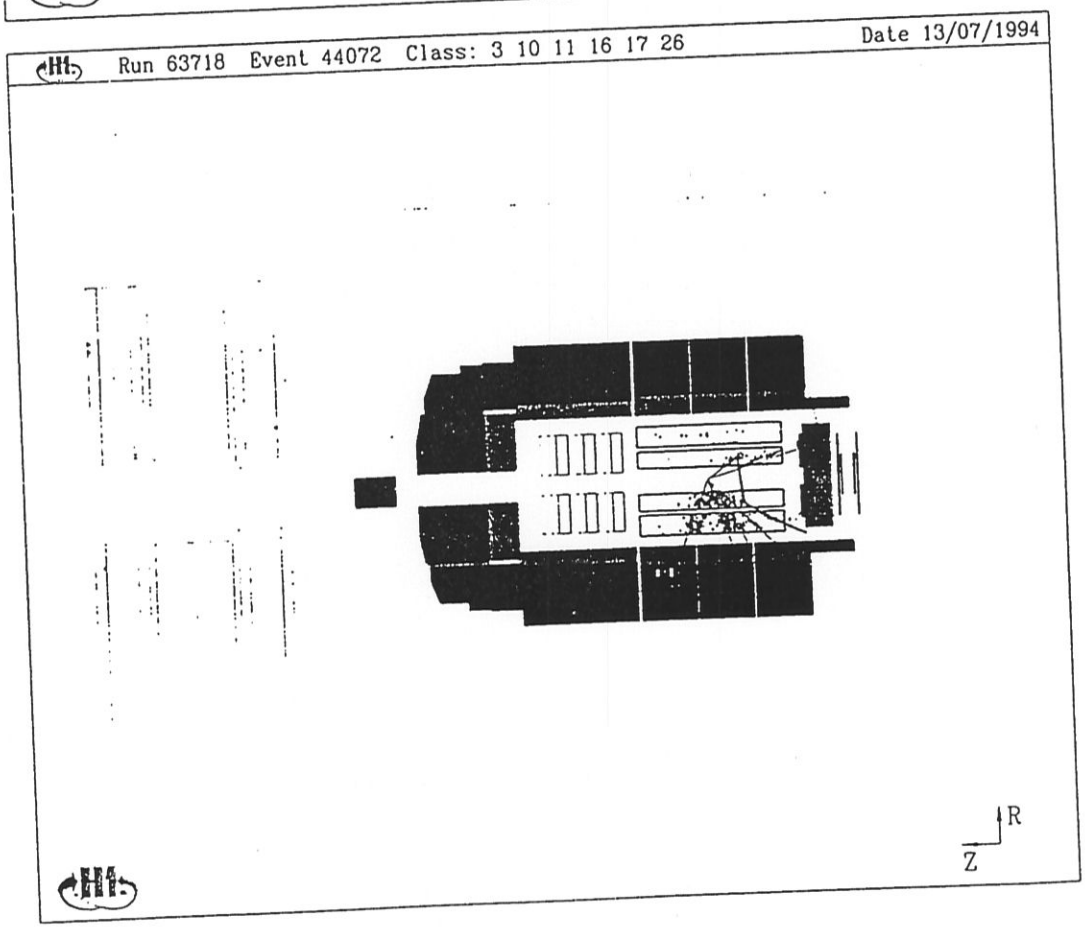
Run 63718 Event 44072 Class: 3 10 11 16 17 26
Date 13/07/1994
R
Z

The Photoproduction Measurement

The measurement is restricted to the kinematic region in which the Electron tagger is efficient:

$$0.3 < y < 0.5 \qquad \Rightarrow \langle W_{\gamma p} \rangle = 187\text{GeV}$$

The γp CMS is boosted in the proton direction by ~ 2 units of rapidity.

- Sensitivity to M_X but not to M_Y.
- The forward detectors give an indication of whether or not the proton dissociates.

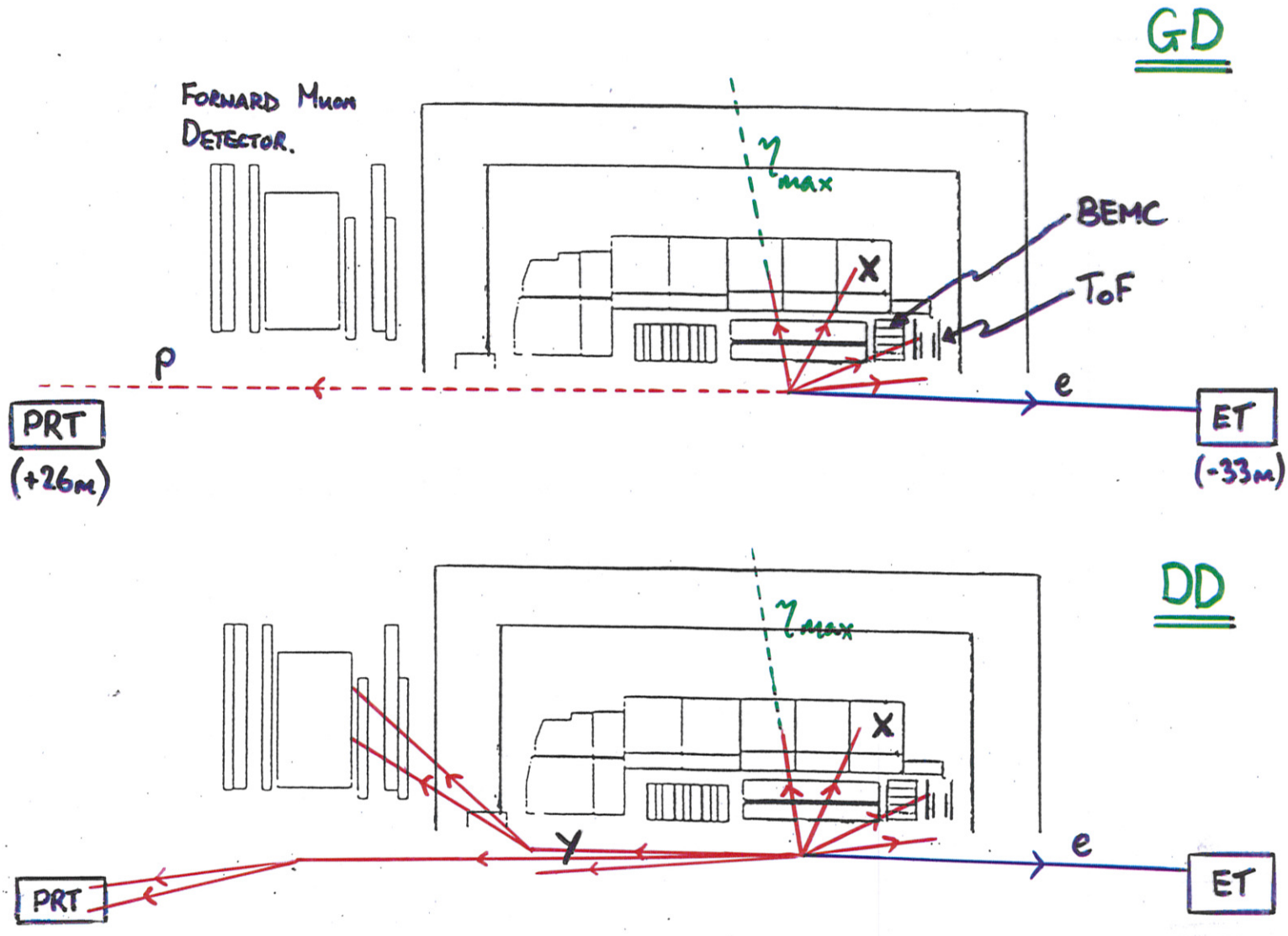

Data Samples

TRIGGER	*NOMINAL VERTEX* ($z_0 = +5$cm)	*SHIFTED VERTEX* ($z_0 = +70$cm)
eTag × *ToF*	$23.2 \pm 0.4\text{nb}^{-1}$	$23.8 \pm 1.3\text{nb}^{-1}$
eTag × *z-vertex*	$22.8 \pm 0.4\text{nb}^{-1}$	

Rejection of Beam-Gas Background

Nominal Vertex z-vertex:

Reconstructed $|z - z_0| < 30$cm.

Nominal Vertex ToF:

If $\exists$ reconstructed vertex, $|z - z_0| < 30$cm.

$E_{LAr} + E_{BEMC} > 1$GeV.

Shifted Vertex ToF:

If $\exists$ reconstructed vertex, $|z - z_0| < 30$cm.

$E_{LAr} + E_{BEMC} > 0.2$GeV.

BPC Hit.

The remaining level of beam-gas background is estimated from pilot-bunch information, and subtracted statistically.

Monte Carlo Models

- Averages of PHOJET and PYTHIA Monte Carlos are used to correct the data.
- Both are based on Regge parameterisations and the VDM.
- Both contain simulations of all four diffractive sub-processes, and non-diffractive events.

In a previous H1 publication Z.Phys. C69(1995) 27, measurements were made of the EL, GD, PD and total γp cross-sections.

These are used to constrain the relative fractions of each sub-process in the Monte Carlos.

$$ND : GD : PD : DD : EL = 0.5 : 0.125 : 0.075 : 0.2 : 0.1$$

Varying the ratio $ND : DD$ has little affect on the results.

Trigger Element Efficiencies

From a Monte Carlo study, taking PHOJET / PYTHIA averages.

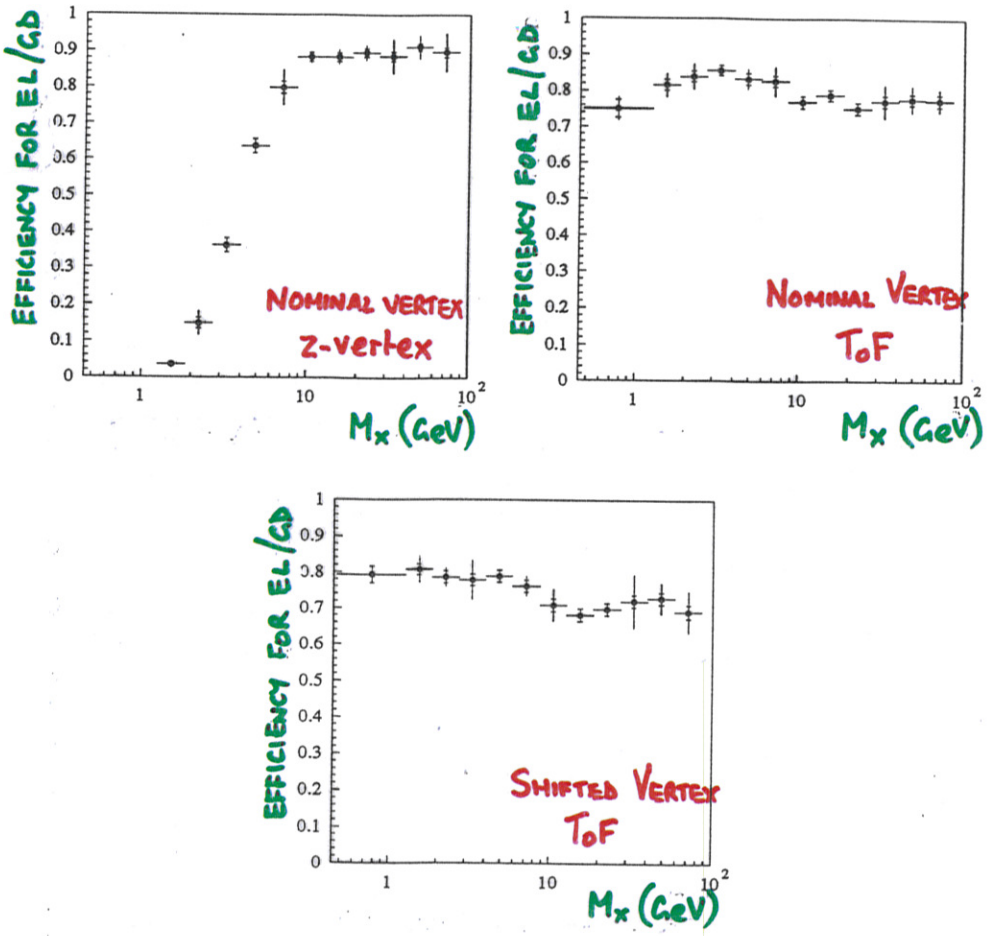

- The ToF trigger data are used for measurements at all M_X.
- The z-vertex trigger data are only used for $M_X \gtrsim 7\text{GeV}$.
- Efficiencies for PD and DD are similar to those for EL and GD.

Reconstruction of the invariant mass, M_X

A mixed reconstruction method is used:

- Isolated low energy calorimeter clusters are rejected as noise.
- The remaining track and calorimeter information is combined in a way that optimises the resolution on the hadronic 4-vector.
- The system, X is taken as all activity backward of the largest rapidity gap in the main detector.

$$\text{Constrain } (p_x, p_y)_h = 0$$

$$\text{Then } M_X^2 = (E - p_z)_h \cdot (E + p_z)_h$$

$$M_X^2 = 2yE_e(E + p_z)_h$$

Insensitive to losses in the backward direction.

Reconstruction Method

SHIFTED VERTEX ToF

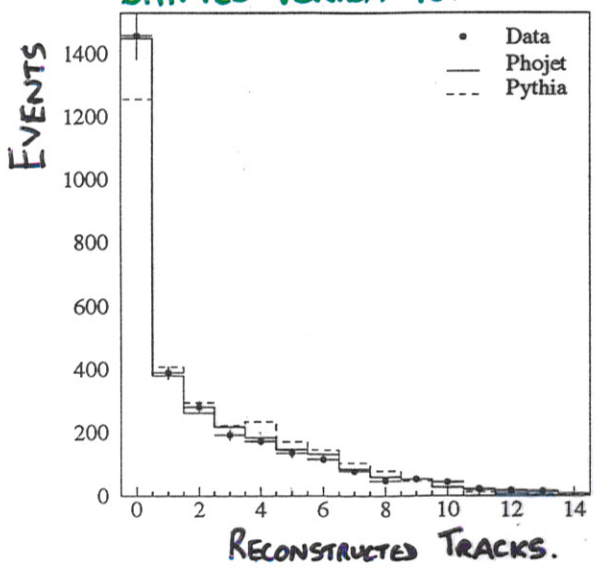

NOMINAL VERTEX z-vertex

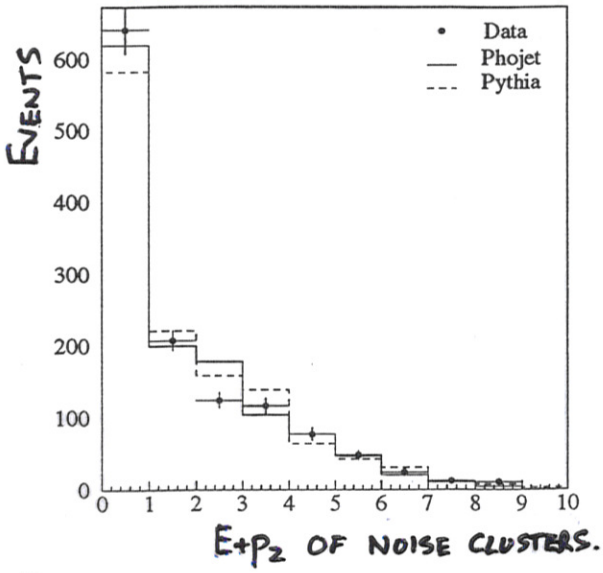

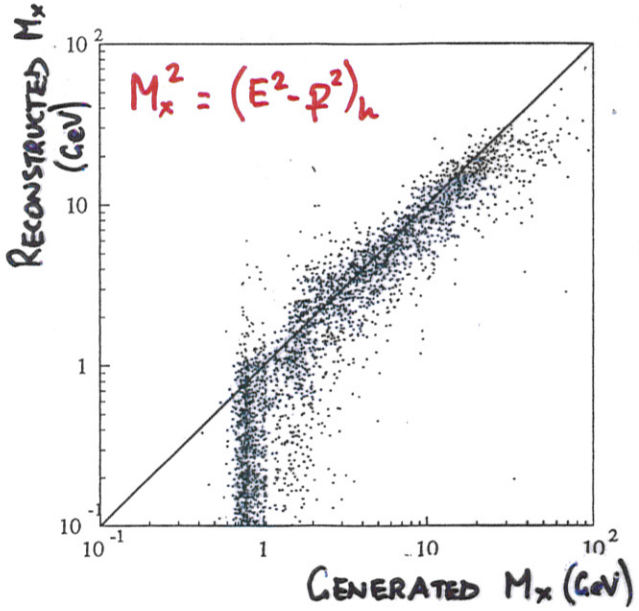

(PHOJET MC)

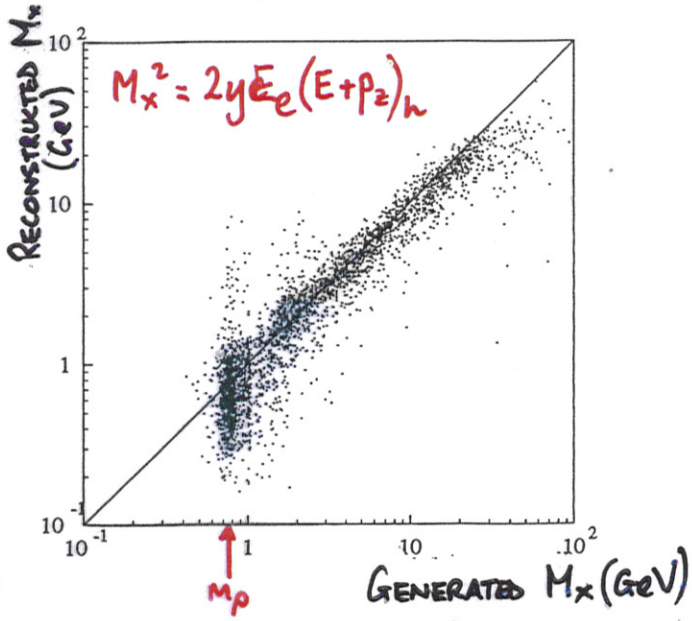

(PHOJET MC)

Selection of EL and GD Diffractive Events

- No signal in the Proton Remnant Tagger.
- No signal in the Forward Muon Detector.
- $\eta_{max} < 3.0$

Selection of PD and DD Diffractive Events

- A signal from the Proton Remnant Tagger, the Forward Muon Detector, or both.
- The largest gap in the main detector must extend to its forward edge.

Allows measurement at low M_X, M_Y only.
Above $M_Y \sim 10$GeV, parts of the system, Y are often observed in the calorimeter.
The PD / DD measurement is corrected to $M_Y < 10$GeV.

Efficiency of the Proton Inelastic Selection

Monte Carlo study using averages of PHOJET and PYTHIA results with PD and DD events.

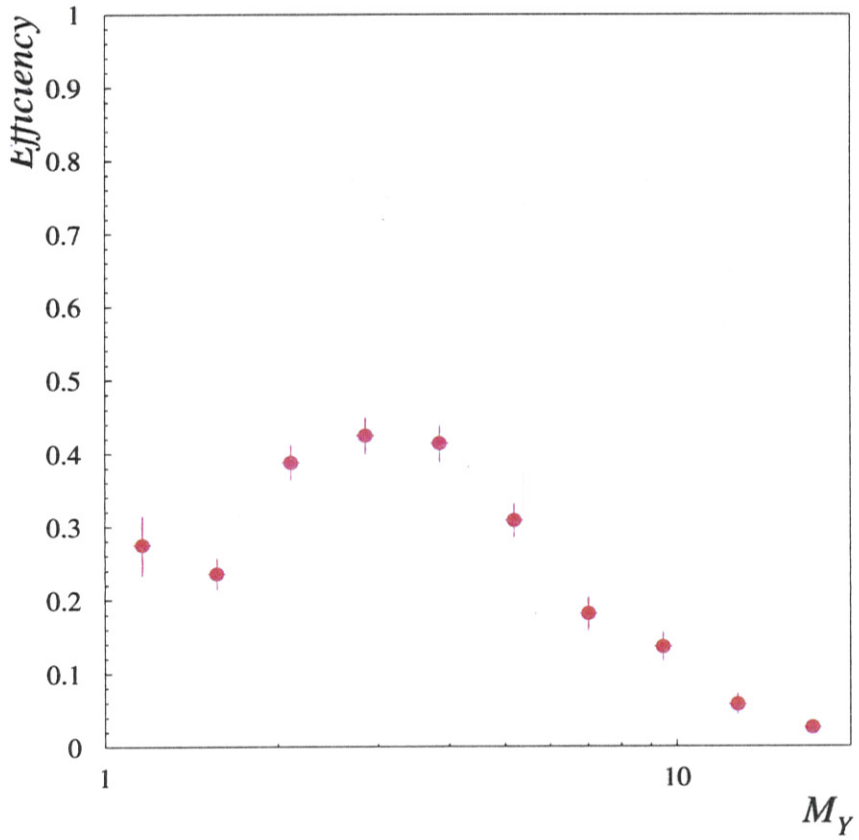

- Sensitivity extends to the lowest lying proton excitations.
- The additional requirement of the central gap reduces non-diffractive background to $\sim 0.5\%$.

Forward Detector Selection

Control plots comparing photoproduction data to Pythia Monte Carlo.

To select non-diffractive events, a cut of $\eta_{max} > 3.2$ is applied.

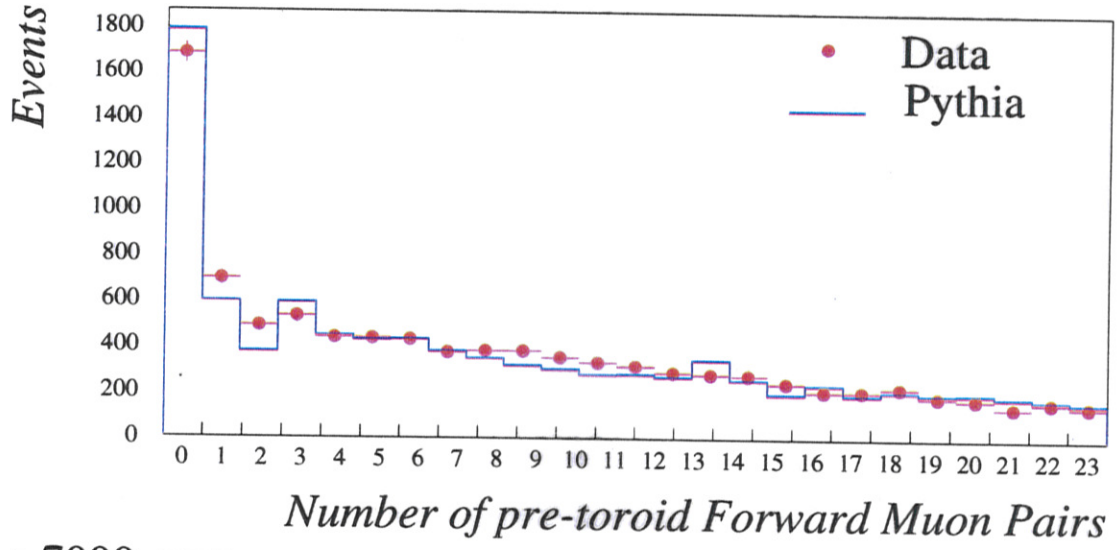

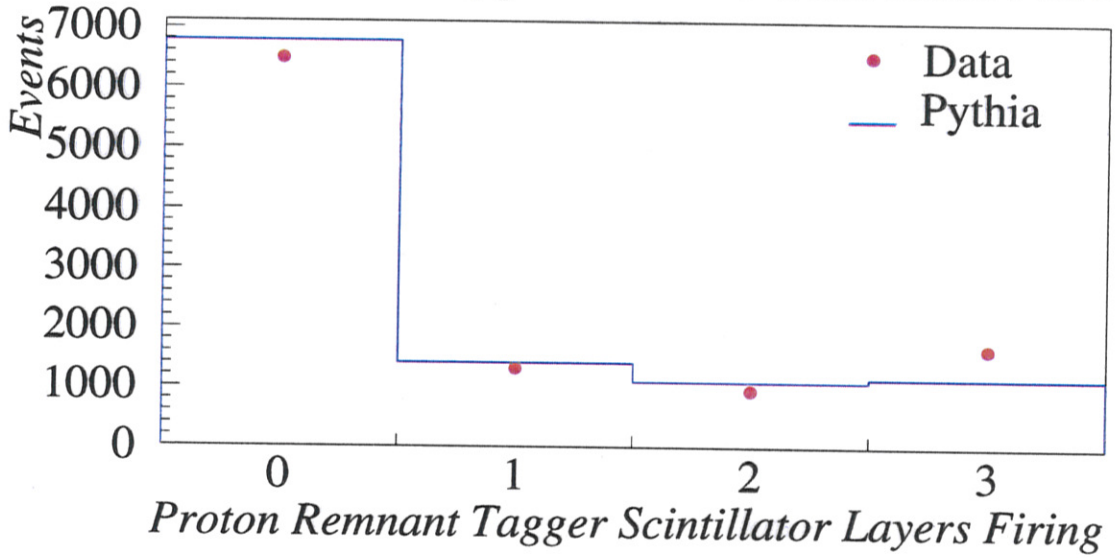

Uncorrected M_X Distributions

Data compared to averages of PHOJET / PYTHIA.

Low mass components of the ToF samples.

GD / EL SELECTION

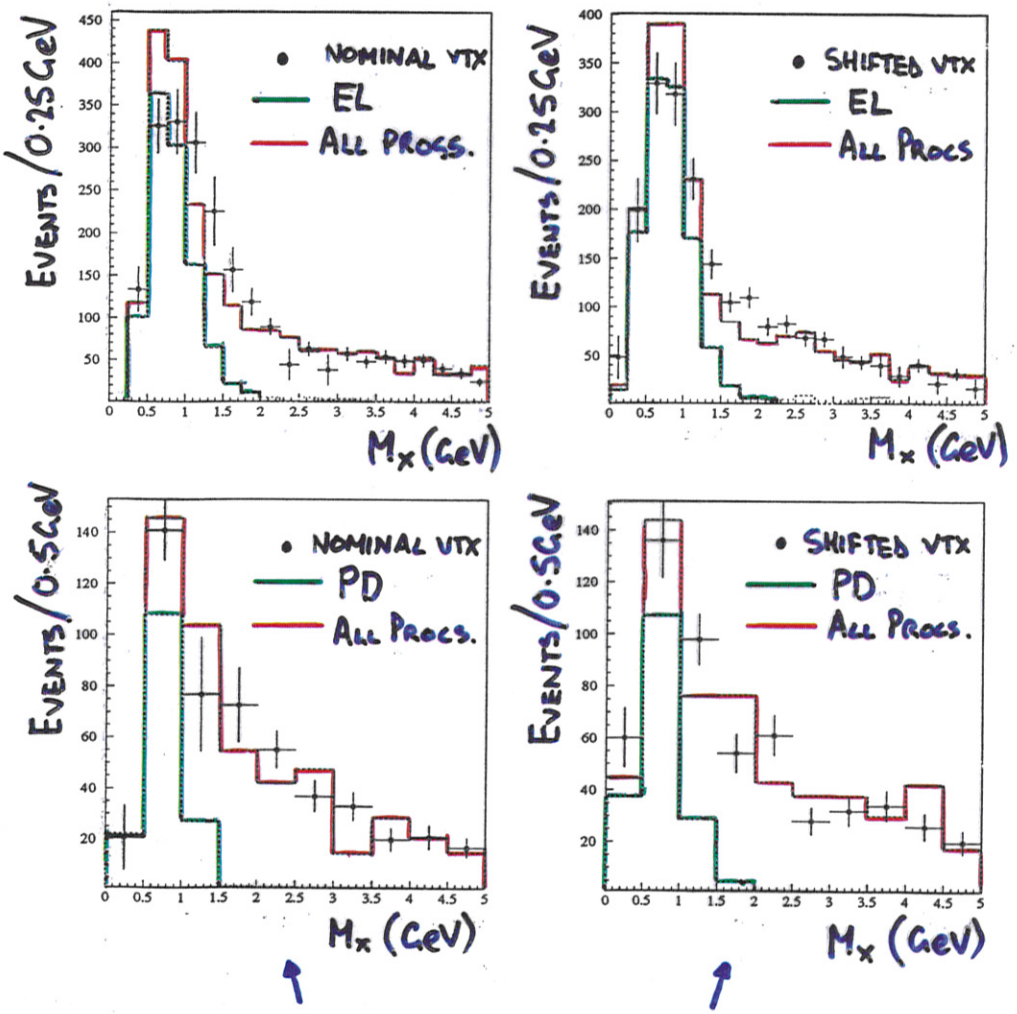

PD / DD SELECTION

Comparison of Points for $\frac{d\sigma(\gamma p \to X p)}{dM_X^2}$

(CORRECTED EL/GD SELECTION)

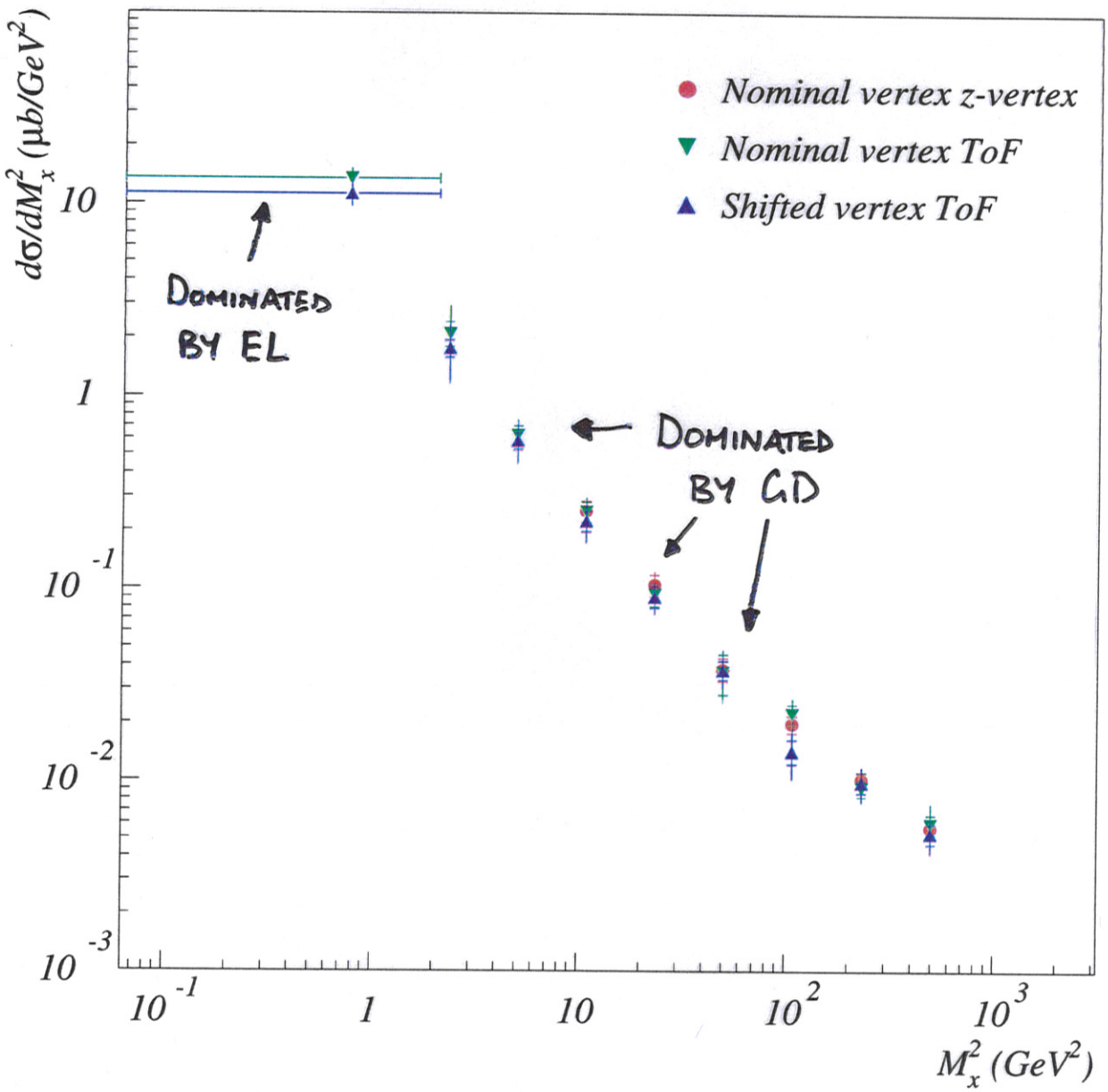

Interpretation of the Cross-Section

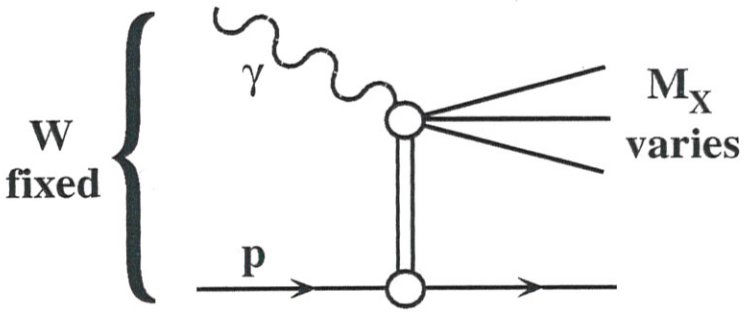

Muller / triple-Regge approach applies.

$$\frac{d^2\sigma}{dM_X^2 dt} \sim \left(\frac{1}{M_X^2}\right)^{\alpha(0)+2\alpha' t}$$

- t is not measured
- Fit data in the triple Regge region, $W^2 \gg M_X^2 \gg t$ to the form

$$\frac{d\sigma}{dM_X^2} = \left(\frac{A}{M_X^2}\right)^n$$

$n = \alpha(0) + 2\alpha' t$?

Cross-Section $\frac{d\sigma}{dM_X^2}$ at $Q^2 = 0$

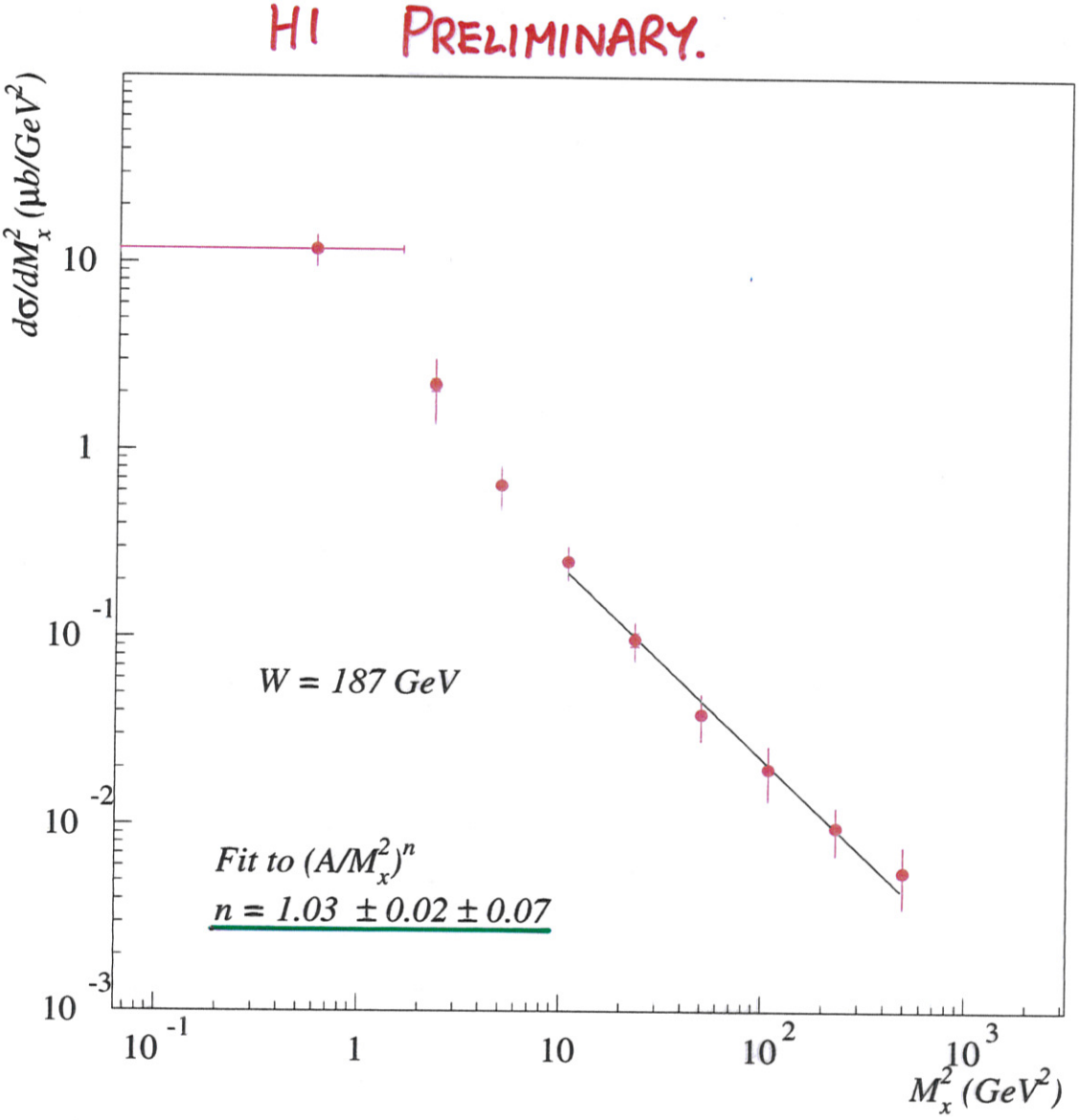

The measured slope is consistent with the leading exchange of the soft pomeron, $\alpha(t) \sim 1.08 + 0.25t$.

Total Cross-Sections at $W_{\gamma p} = 187\text{GeV}$

The Monte Carlos are used to unfold total diffractive cross-sections from the differential cross-sections in the measured kinematic range.

All results are preliminary.

EL (With $V = \rho, \omega, \phi$)

$$\sigma(\gamma p \to Vp) = 16.7 \pm 0.9(stat) \pm 2.8(sys)\mu\text{b}$$

GD (Corrected to $\frac{M_X^2}{W_{\gamma p}^2} (\sim x_{I\!P}) < 0.05$)

$$\sigma(\gamma p \to Xp) = 21.5 \pm 0.6(stat) \pm 5.9(sys)\mu\text{b}$$

PD (For $M_Y < 10\text{GeV}$)

$$\sigma(\gamma p \to VY) = 6.5 \pm 0.6(stat) \pm 1.0(sys)\mu\text{b}$$

Extrapolating to $\frac{M_Y^2}{W_{\gamma p}^2} < 0.05$

$$\sigma(\gamma p \to VY) = 9.8 \pm 0.9(stat) \pm 2.5(sys)\mu\text{b}$$

DD (For $M_X < 5.8\text{GeV}$, $M_Y < 10\text{GeV}$)

$$\sigma(\gamma p \to XY) = 14.2 \pm 0.5(stat) \pm 3.6(sys)\mu\text{b}$$

- The results are consistent with the previous measurement Z.Phys. C69(1995) 27, and errors are reduced.

Conclusions for Photoproduction

- Cross-sections for the EL, GD and PD diffractive sub-processes in photoproduction have been measured at $W = 187\text{GeV}$.
- The DD cross-section has been measured in a highly limited kinematic range.
- A lower limit of 37% can be set for the diffractive fraction of the total cross-section. (c.f. $\sim 10\%$ at large Q^2.)
- The invariant mass distribution, $\frac{d\sigma}{dM_X^2}$, of processes that are elastic at the proton vertex has been measured.
- A strong elastic peak consistent with vector dominance is observed.
- The high mass continuum shows no evidence for deviations from soft pomeron dynamics.

Deep Inelastic Diffraction

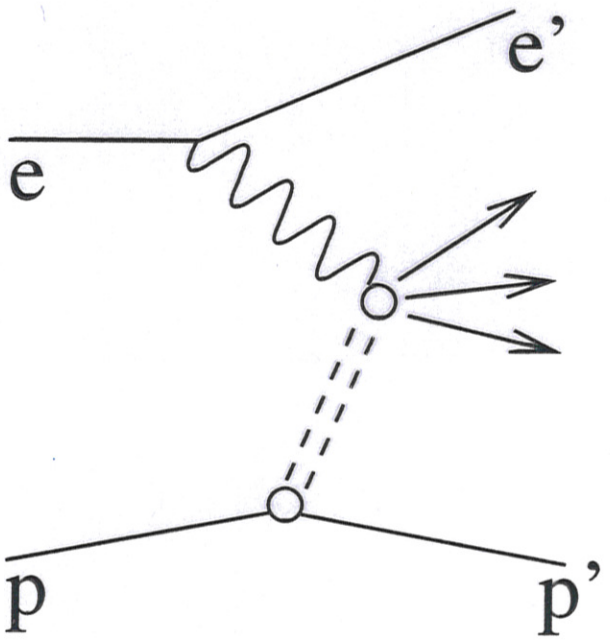

Probing the structure of the diffractive exchange.

Preliminary 1994 results, following on from
Phys. Lett. 348(1995) 681.

Definition of the Measured Cross Section

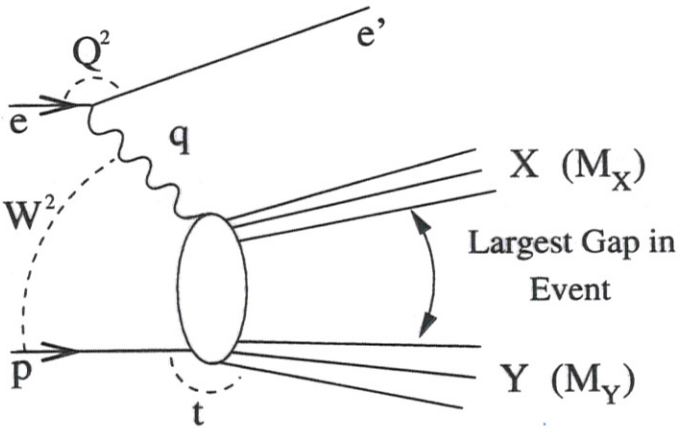

Systems X and Y are separated by the largest rapidity gap in the hadronic final state.

Kinematics are defined in terms of the systems X and Y:

$$\beta = \frac{Q^2}{2q.(P-Y)} \simeq \frac{Q^2}{Q^2+M_X^2}$$

$$x_{I\!P} = \frac{q.(P-Y)}{q.P} \simeq \frac{Q^2+M_X^2}{Q^2+W^2}$$

such that $x = \beta\, x_{I\!P}$.

These definitions are completely general, and can also be applied to non-diffractive processes.

In models based on pomeron exchange:

$$\beta = x_{q/I\!P}$$

$$x_{I\!P} = x_{I\!P/p}$$

Definition of $F_2^{D(3)}(x, Q^2, x_{I\!P})$

The measured cross-section is defined as:

$$\frac{d^3\sigma(ep \to eXY)}{dx dQ^2 dx_{I\!P}} = \frac{4\pi\alpha^2}{xQ^4}\left(1 - y + \frac{y^2}{2}\right) F_2^{D(3)}(x, Q^2, x_{I\!P})$$

- R is at present unmeasured. $\rightarrow$ We set it to 0.
- We have no sensitivity to t.
- M_Y is not measured, but is forced to be small.

Definition of the Measured Cross-Section

Experimentally, we select diffractive events by requiring an absence of activity in the laboratory rapidity range, $3.4 < \eta < 7.0$.

This limits the measurement to $x_{I\!P} < 0.05$ and $M_Y < 1.6$ GeV.

All results and cross sections quoted refer to this kinematic region.

- This ensures that M_X and $x_{I\!P}$ are well reconstructed.
- Proton dissociation models (PYTHIA, PHOJET, DIFFVM) indicate that the correction from $M_Y < 1.6$GeV to an elastic cross-section is $\simeq 5\%$.

Selection of Diffractive DIS Events

Require:

- An electron cluster in the Backward Electromagnetic Calorimeter with $E' > 8$ GeV
- At least one reconstructed track pointing to the interaction region
- No reconstructed signal in all sub-detectors that reach $\eta > 3.4$.

From 2.0 pb^{-1} of 1994 data, $\sim 20,000$ events are selected.
This represents an increase of over a factor of 10 in statistics compared to the 1993 measurement.

In addition 0.06 pb^{-1} of data are used with the vertex shifted by 65 cm in the proton beam direction, allowing access to lower values of Q^2.

Monte Carlos

Used to correct for experimental bias (acceptance and smearing).

- Background to the diffractive sample arises from events that are reconstructed with $x_{I\!P} < 0.05$ and $M_Y < 1.6\text{GeV}$, but *actually* have $x_{I\!P} > 0.05$ or $M_Y > 1.6\text{GeV}$.
- The diffractive Monte Carlo has a structure function input consistent with that measured.
- All Monte Carlo simulations include QCD evolution and QED radiation effects.

Monte Carlos

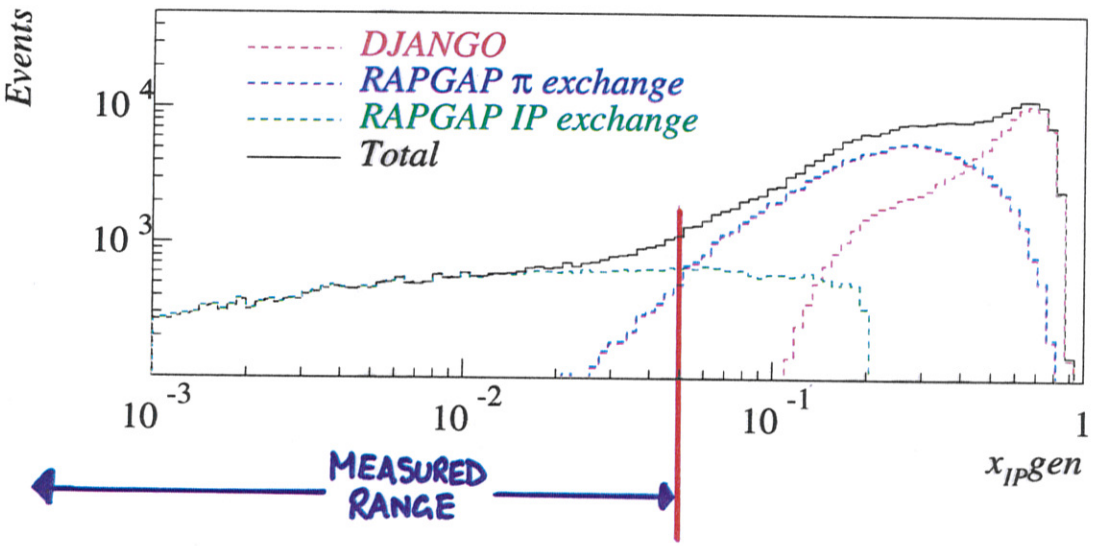

Monte Carlos are mixed in order to best reproduce control distributions before any diffractive selection:

- 17 % RAPGAP $I\!P$ $(0 < x_{I\!P} < 0.2)$
- 46 % RAPGAP π $(0 < x_{I\!P} < 1)$
- 0.4% DIFFVM (ρ^0, ω, ϕ)
- 37 % DJANGO Non-Diffractive

  $(x_{I\!P} > 0.1$ or $M_Y > 1.6\text{GeV})$

Replacing the RAPGAP π Monte Carlo with a larger proportion of DJANGO has little effect on the results.

Kinematic Reconstruction

The same method of reconstruction of the 4-vector of the system, X, is used as in the photoproduction case.

- Combined track and calorimetry information.
- Noise suppression.

The best reconstruction is obtained from

$$M_X^2 = (E^2 - \underline{p}^2)_h .$$

The remaining kinematics are obtained by the Σ method:

$$\Sigma = (E - p_z)_h$$

$$y = \frac{\Sigma}{\Sigma + E_{e'}(1 - \cos\theta_e)}$$

$$Q^2 = \frac{E_{e'}^2 \sin^2\theta_e}{1 - y}$$

$$x = \frac{E_{e'}}{E_p} \frac{\cos^2\frac{\theta_e}{2}}{y}$$

This method provides good reconstruction over the entire kinematic range, and substantially reduces radiative corrections.

Reconstruction of Kinematic Quatities (from RAPGAP MC)

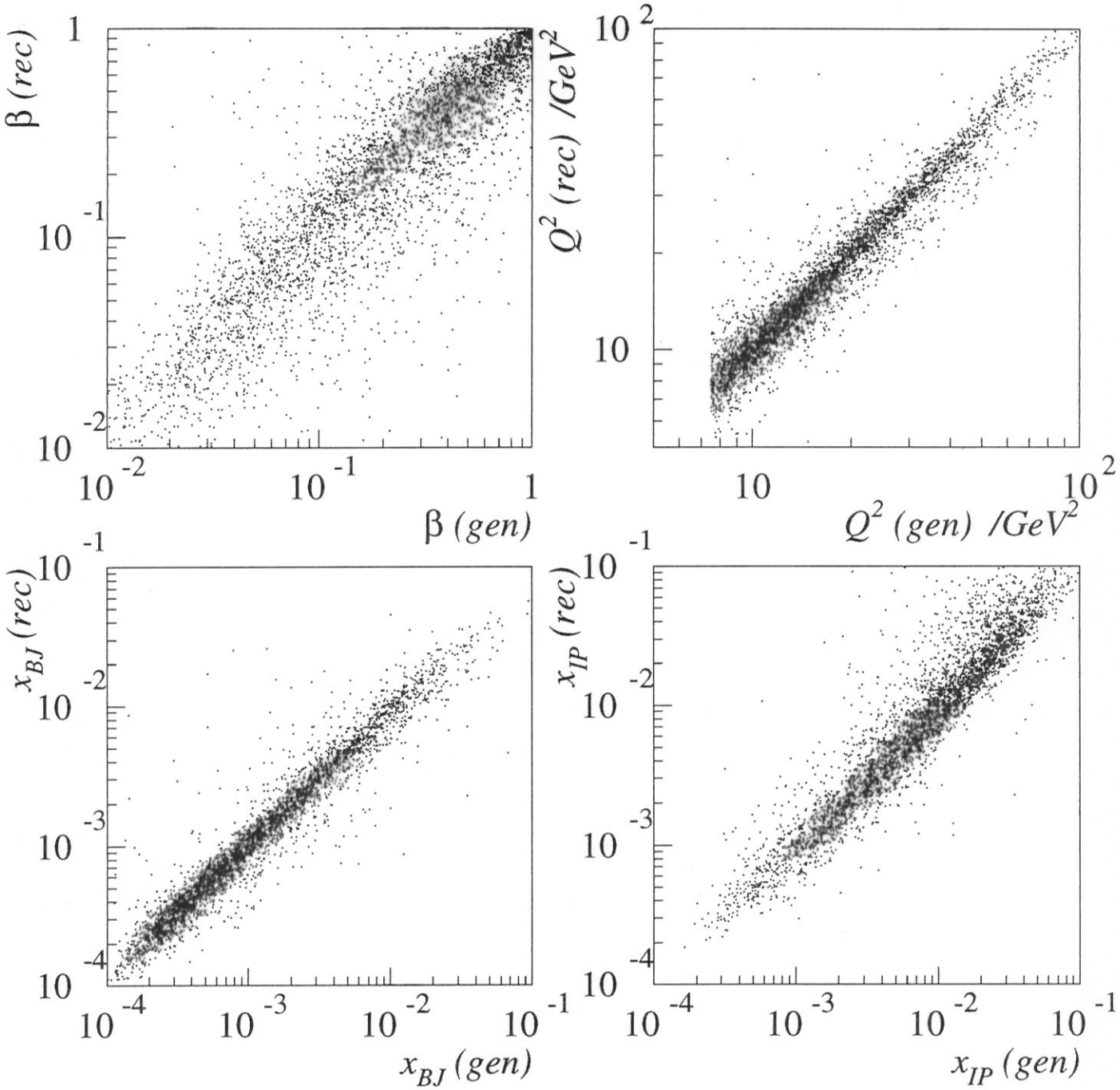

Control Plots

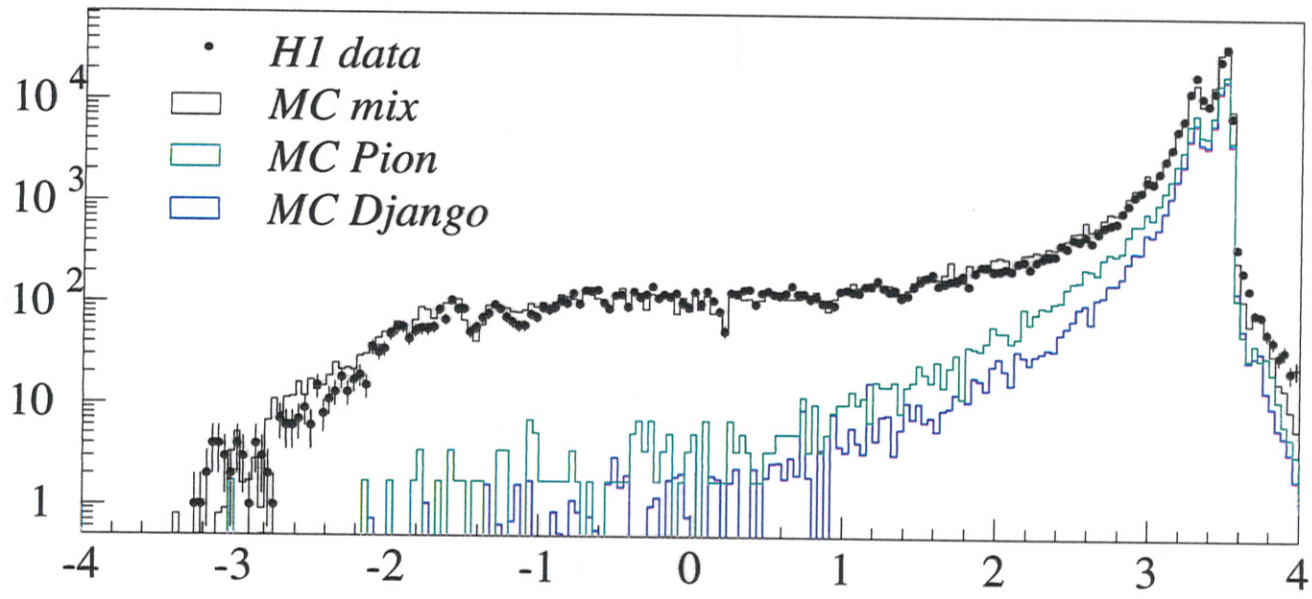

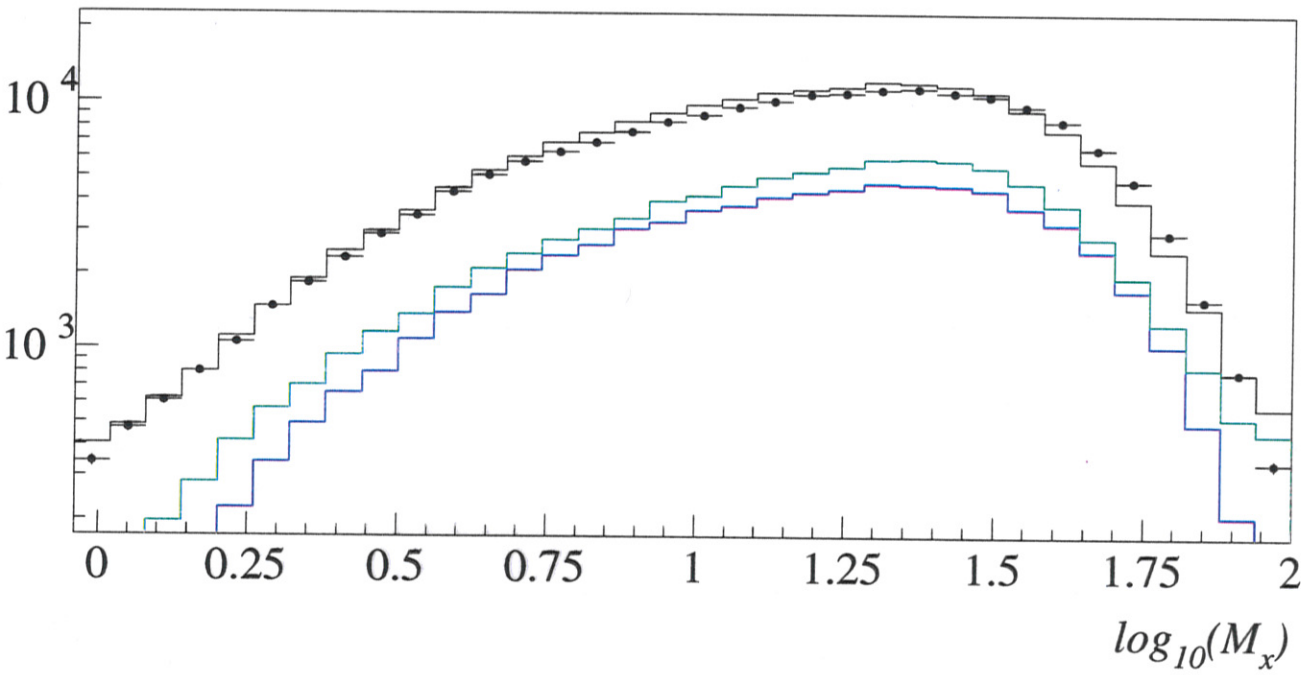

NO DIFFRACTIVE SELECTION.

Control Plots

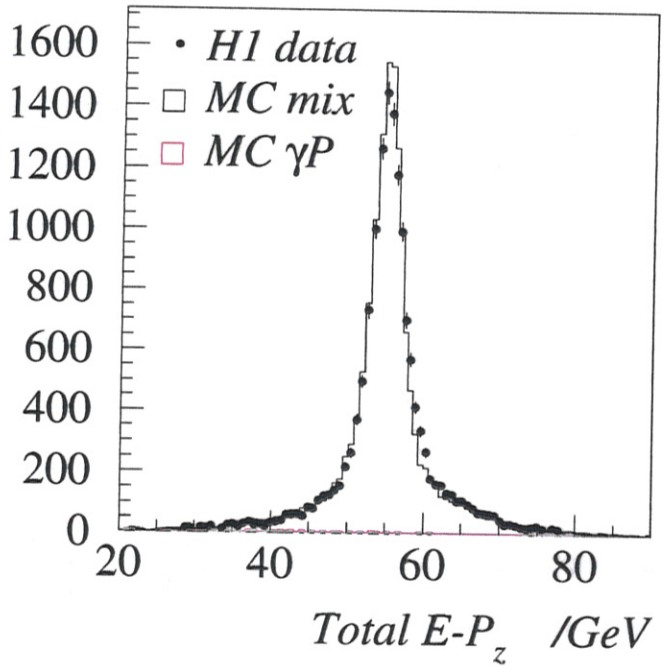

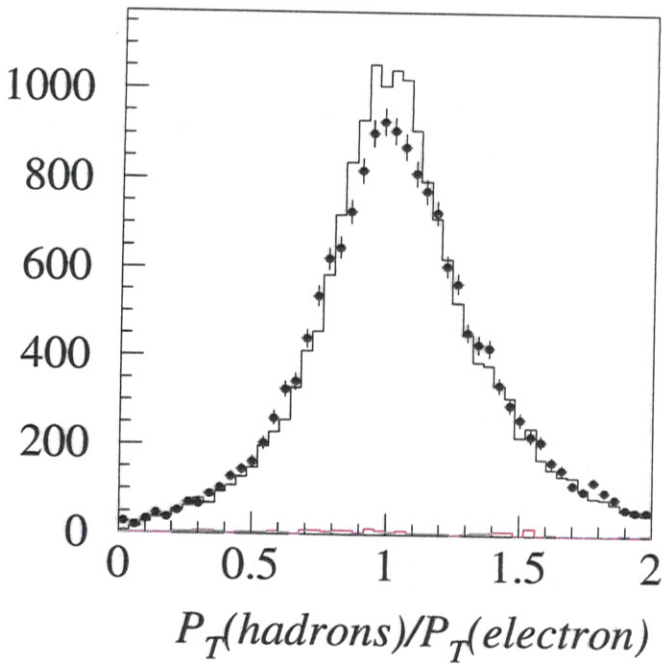

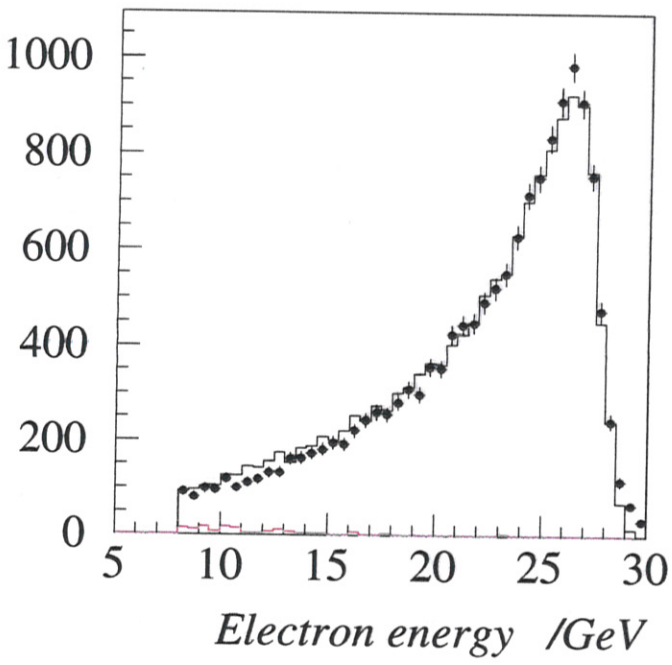

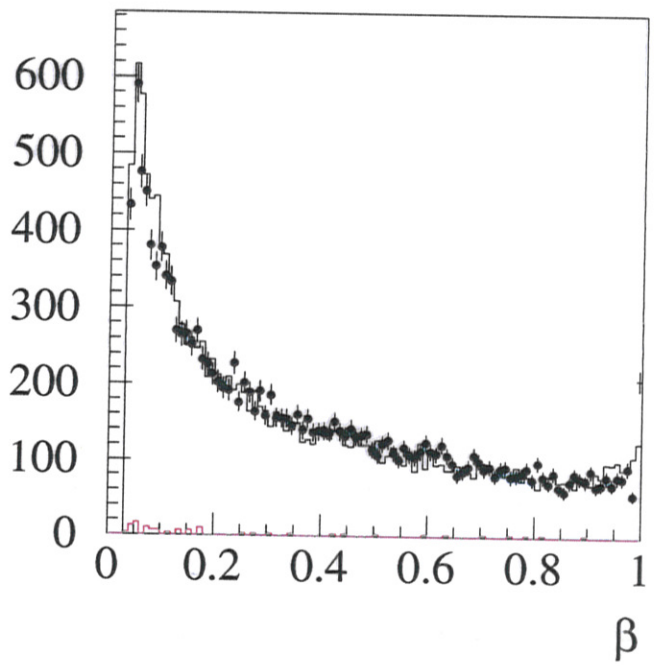

AFTER DIFFRACTIVE SELECTION.

Kinematic Range of the Measurement

$$2.5 < Q^2 < 65\text{GeV}^2$$
$$0.01 < \beta < 0.9$$
$$10^{-4} < x_{I\!P} < 0.05$$

- All bin sizes are smaller than resolutions.
- All bins have acceptance > 0.3
- All bins have purity > 0.2
- All bins have background from high $x_{I\!P}$ or $M_Y < 20\%$.

Systematic Error Anaysis

Systematic errors are derived bin by bin.
The table below shows bin-averaged values.

Source	Method	Mean Error
LAr Energy Scale	$\pm$ 5 %	3 %
Bemc Hadronic Scale	$\pm$ 20 %	3 %
Bemc EM Scale	$\pm$ 1.5 %	5 %
Track Energy Scale	$\pm$ 3 %	6 %
θ_e	$\pm$ 1 mrad	2 %
t Dependence	$\exp 4 \pm 2t$	4 %
$x_{I\!P}$ Dependence	$x_{I\!P}^{-1.1\pm0.2}$	3 %
β Dependence	$\lvert(1/g - g)\beta + g\rvert$ $g = ^{0.75}_{1/0.75}$	3 %
high $x_{I\!P}$ BG	50 %	4 %
γp BG	50 %	0.1 %
Acceptance	MC statistics /model dependence	14 %
Total systematic error		22 %
Total statistical error		20 %

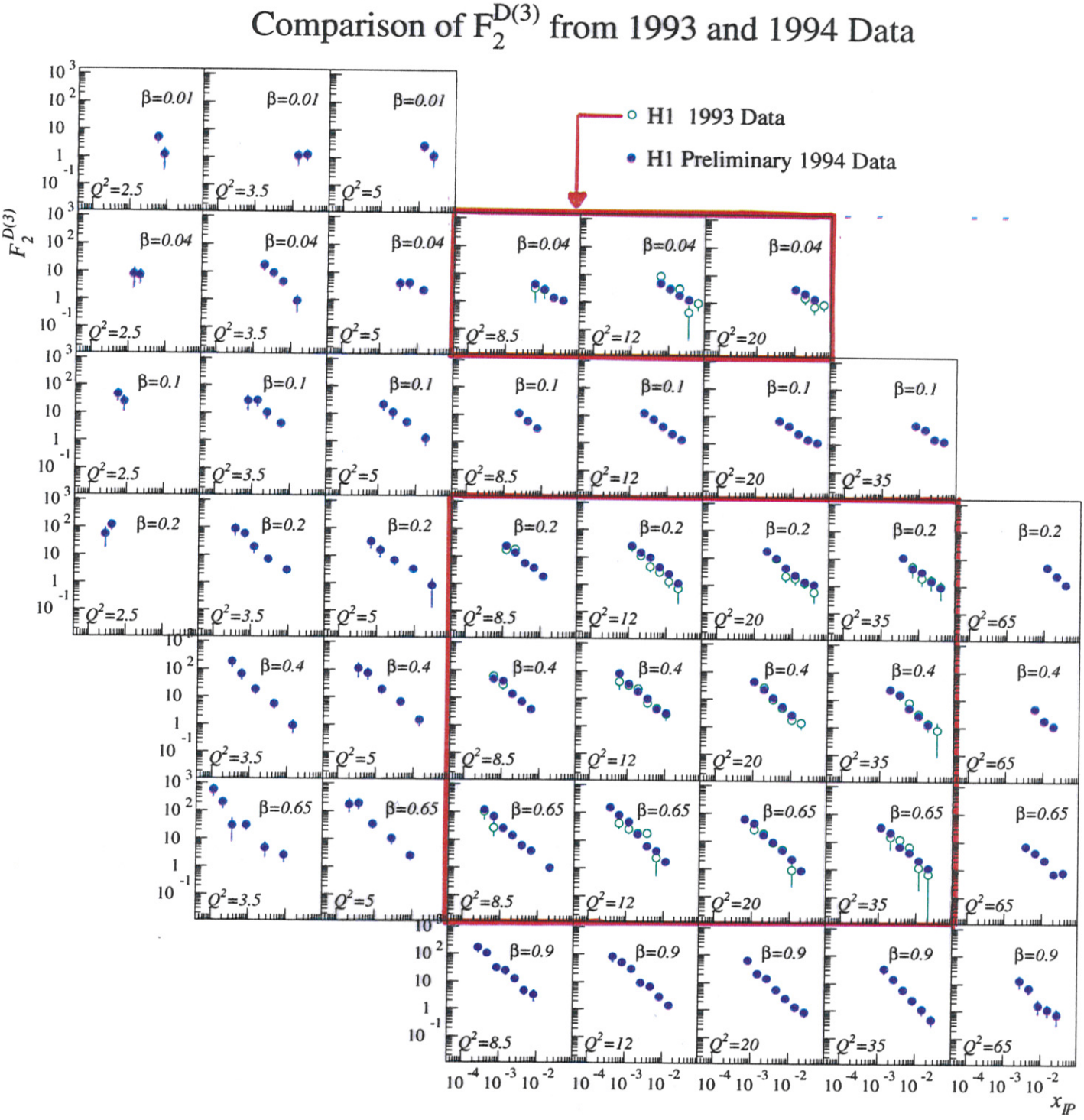

1993: 15 BINS IN β-Q^2.

1994: 43 BINS IN β-Q^2.

CROSS CHECKS for Q^2=12 GeV^2

H1 Preliminary data

NOTICE RE-SCALING

- *Standard selection*
- *Double Angle*
- *Electron Only*
- *M_x From Calo Only*
- *$\eta_{max} < 3$*
- *Only Forward Detectors*
- *No Gap Selection* !!!

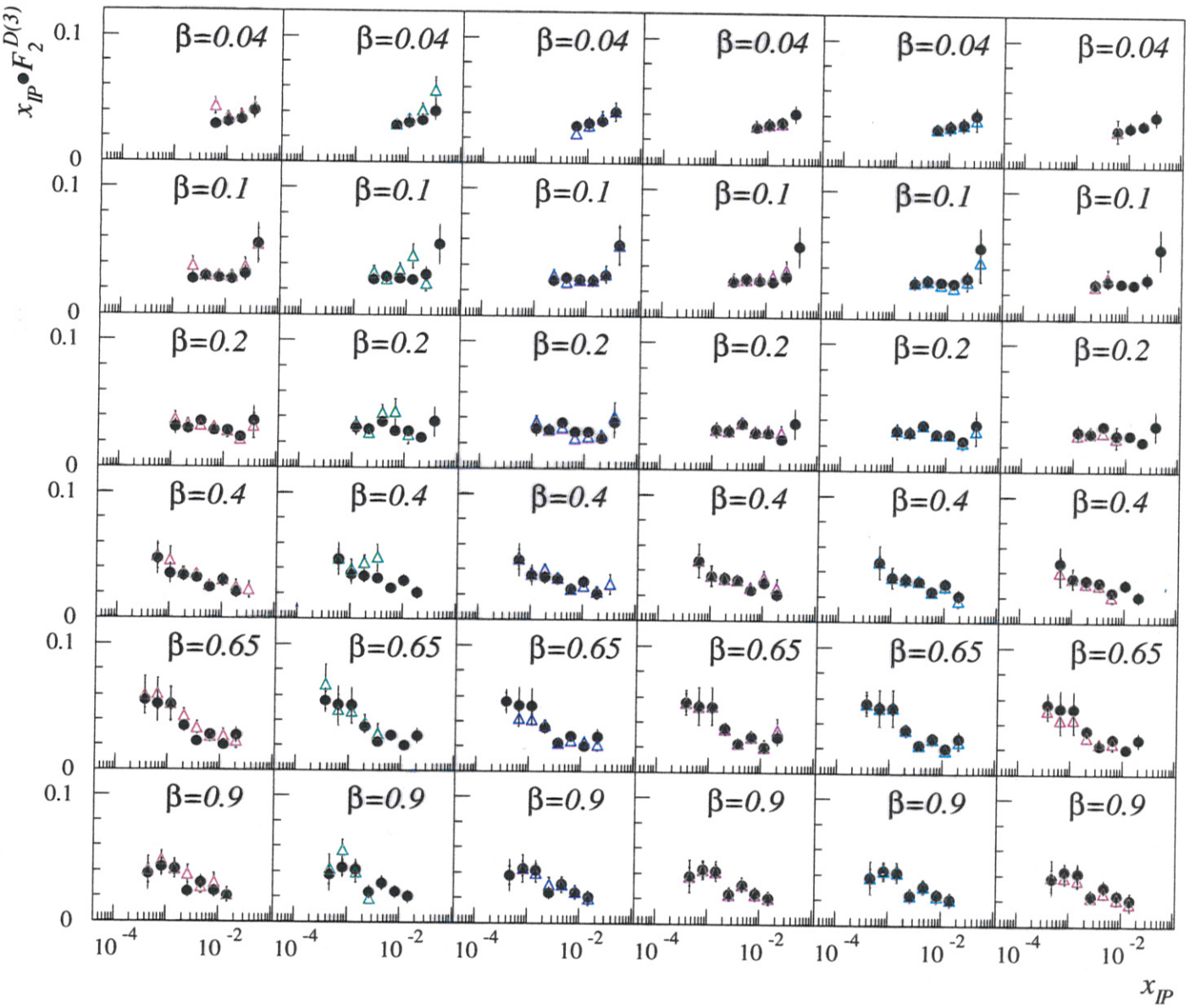

H1 Preliminary $F_2^{D(3)}(\beta, Q^2, x_{I\!P})$

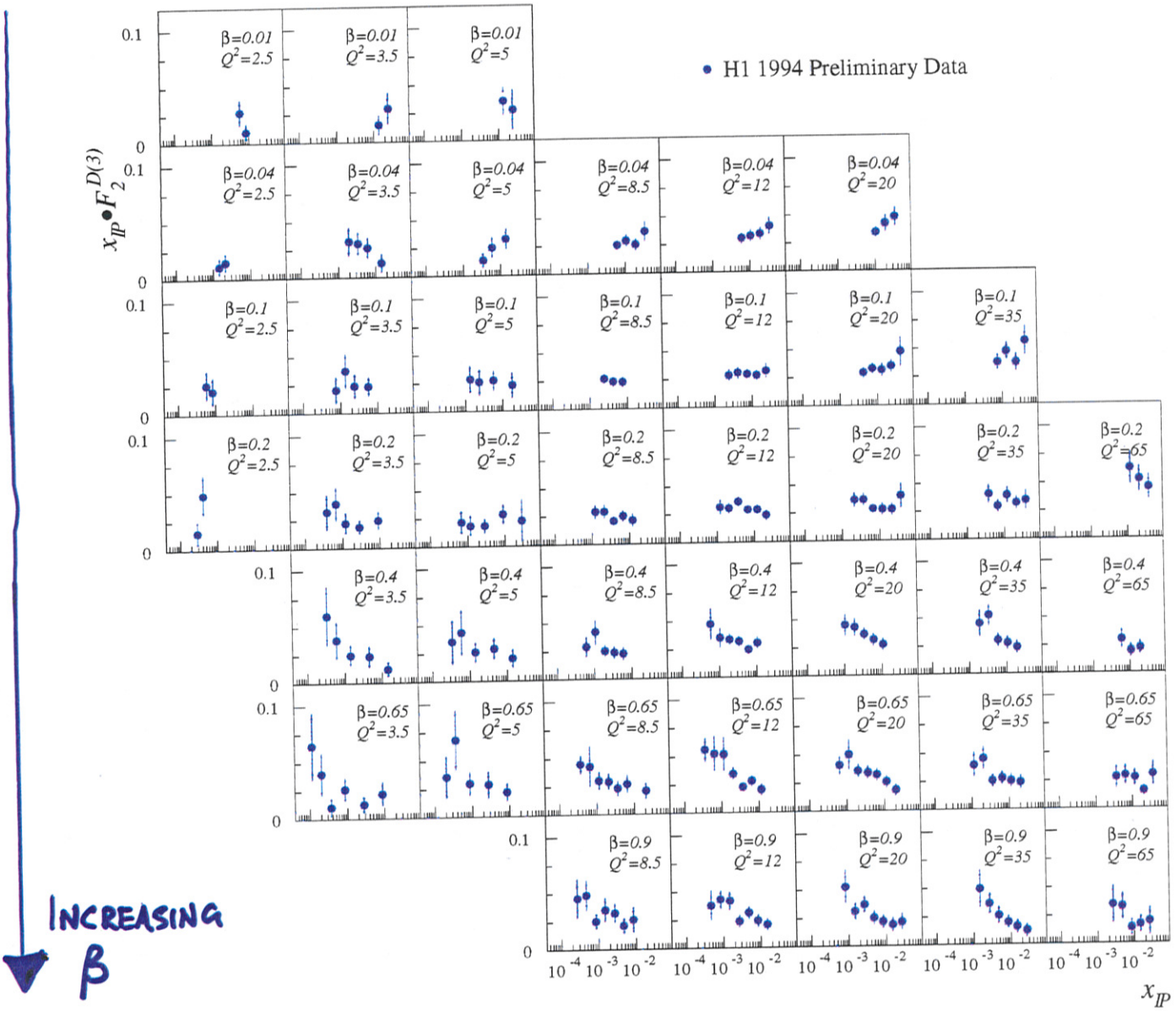

INCREASING β

INCREASING Q^2

Testing Factorisation

The factorisation hypothesis may be stated as:

$$F_2^{D(3)} = A(\beta, Q^2) \cdot f(x_{I\!P})$$

This is tested by fitting the data with a parameterisation

$$F_2^{D(3)} = A(\beta, Q^2) \cdot \frac{1}{x_{I\!P}^n}$$

and allowing n to vary as a function of β or Q^2.

Regge Interpretation

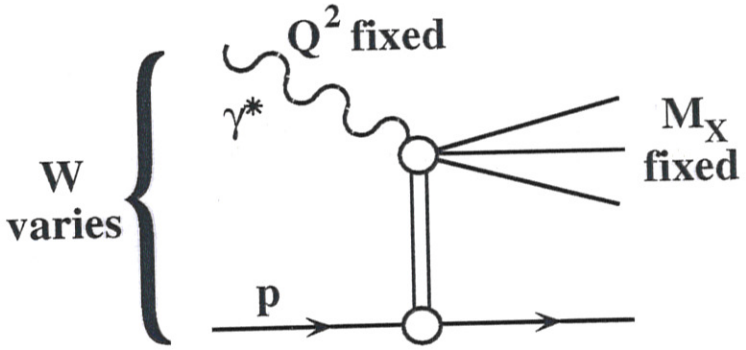

Single Regge parameterisation applies.

At fixed t, $n = 2\alpha(t) - 1$

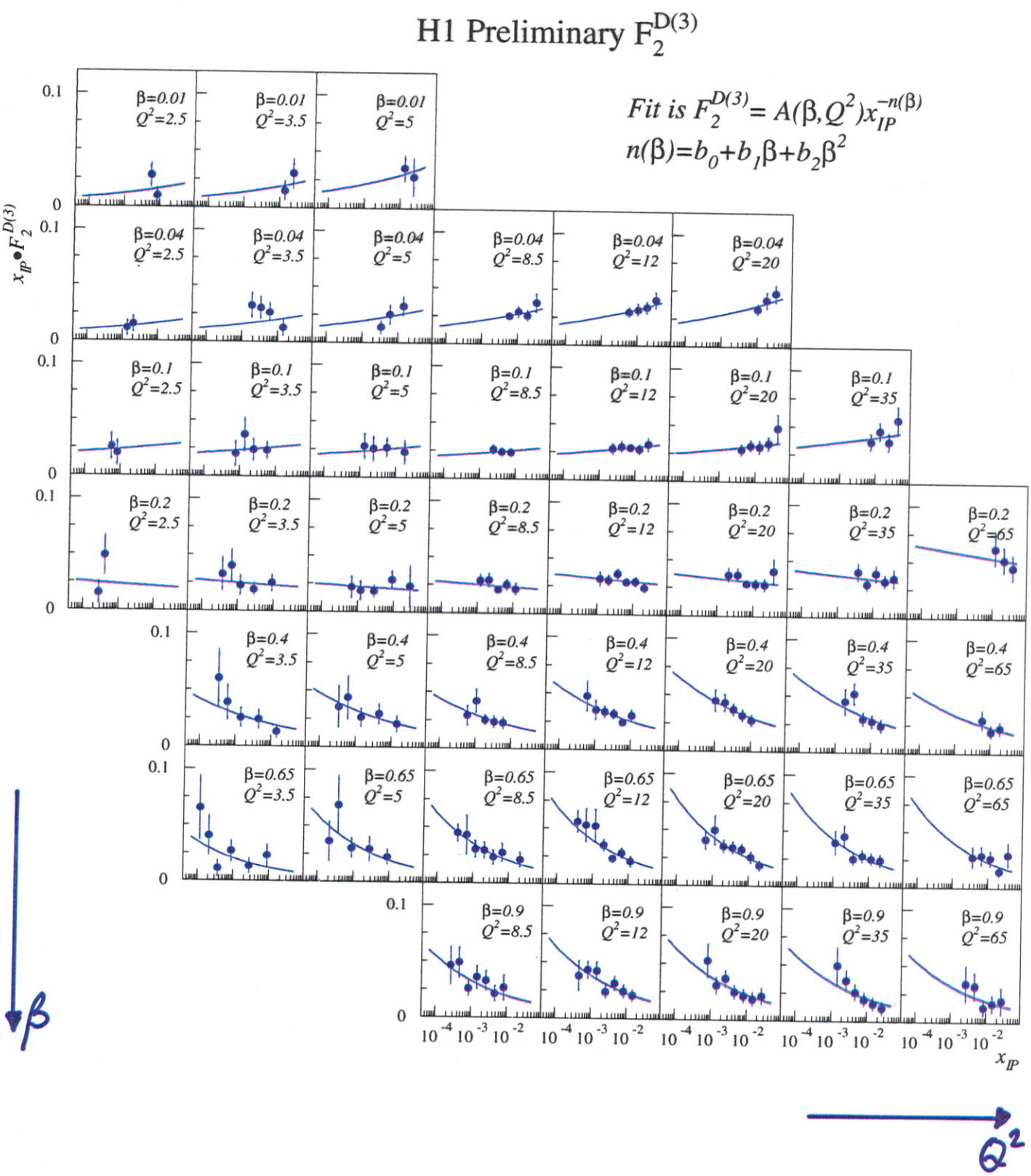
H1 Preliminary $F_2^{D(3)}$
Fit is $F_2^{D(3)} = A(\beta, Q^2) x_{IP}^{-n(\beta)}$
$n(\beta) = b_0 + b_1\beta + b_2\beta^2$
$x_{IP} \bullet F_2^{D(3)}$
x_{IP}
β
Q^2
β=0.01 Q²=2.5
β=0.01 Q²=3.5
β=0.01 Q²=5
β=0.04 Q²=2.5
β=0.04 Q²=3.5
β=0.04 Q²=5
β=0.04 Q²=8.5
β=0.04 Q²=12
β=0.04 Q²=20
β=0.1 Q²=2.5
β=0.1 Q²=3.5
β=0.1 Q²=5
β=0.1 Q²=8.5
β=0.1 Q²=12
β=0.1 Q²=20
β=0.1 Q²=35
β=0.2 Q²=2.5
β=0.2 Q²=3.5
β=0.2 Q²=5
β=0.2 Q²=8.5
β=0.2 Q²=12
β=0.2 Q²=20
β=0.2 Q²=35
β=0.2 Q²=65
β=0.4 Q²=3.5
β=0.4 Q²=5
β=0.4 Q²=8.5
β=0.4 Q²=12
β=0.4 Q²=20
β=0.4 Q²=35
β=0.4 Q²=65
β=0.65 Q²=3.5
β=0.65 Q²=5
β=0.65 Q²=8.5
β=0.65 Q²=12
β=0.65 Q²=20
β=0.65 Q²=35
β=0.65 Q²=65
β=0.9 Q²=8.5
β=0.9 Q²=12
β=0.9 Q²=20
β=0.9 Q²=35
β=0.9 Q²=65
0.1
0
10^{-4} 10^{-3} 10^{-2}

Possible Explanations for Factorisation Breaking

- Different behaviour of the pomeron flux for 'sea' and 'valence' components of the structure function (c.f. Nikolaev Zakharov).
- A contribution from other trajectories (f, π etc.) becoming more significant at low β.
- Higher order pomeron exchange.
-
-
-
-

Structure function of the Colourless Exchange

Define:

$$\tilde{F}_2^D(Q^2,\beta) = \int_{x_{I\!P_L}}^{x_{I\!P_H}} F_2^{D(3)}(Q^2,\beta,x_{I\!P})\,dx_{I\!P}$$

- $x_{I\!P_L} = 0.0003$, $x_{I\!P_H} = 0.05$ are chosen to correspond to the experimentally accessed range.
- The parameterisation of $F_2^{D(3)}$ is used to extrapolate to unmeasured regions.
- In factorisation models,

  $$\tilde{F}_2^D(Q^2,\beta) \propto F_2^{I\!P}(Q^2,\beta)$$

  where $F_2^{I\!P}(Q^2,\beta)$ is the pomeron structure function.
- If factorisation is broken, $\tilde{F}_2^D(Q^2,\beta)$ remains well defined, and may be interpreted as a structure function for the colourless exchange, averaged over $x_{I\!P}$ and t.

$\tilde{F}_2^D(\beta, Q^2)$

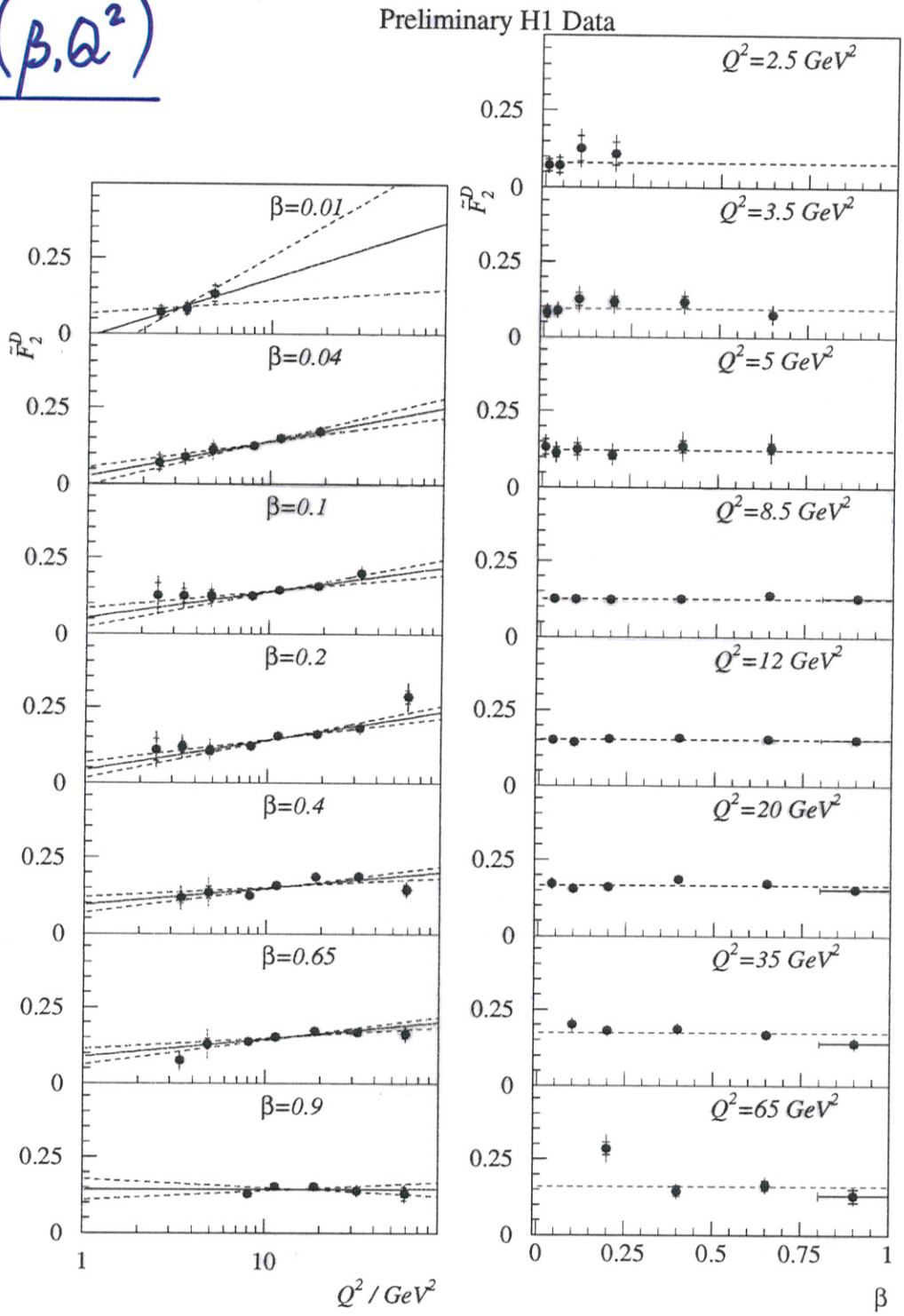

- $\tilde{F}_2^D(Q^2, \beta)$ shows a flat β distribution.
- Clear evidence is seen for scaling violations.
- A rise with $\log(Q^2)$ persists to the largest values of β.

QCD Analysis of $\tilde{F}_2^D(\beta, Q^2)$

- Consider light quark flavour singlet $(u + \bar{u} + d + \bar{d} + s + \bar{s})$ + gluon
- Parameterise at $Q_0^2 = 2.5\,\mathrm{GeV}^2$:

$$x_{i/\mathbb{P}} f_i(x_{i/\mathbb{P}}) = A_i x_{i/\mathbb{P}}^{B_i} (1 - x_{i/\mathbb{P}})^{C_i}$$

- Solve DGLAP evolution equations to evolve parton densities to higher Q^2 and fit A_i, B_i, C_i to data (i=singlet,gluon)
- Charm included via photon–gluon fusion

H1 Preliminary 1994

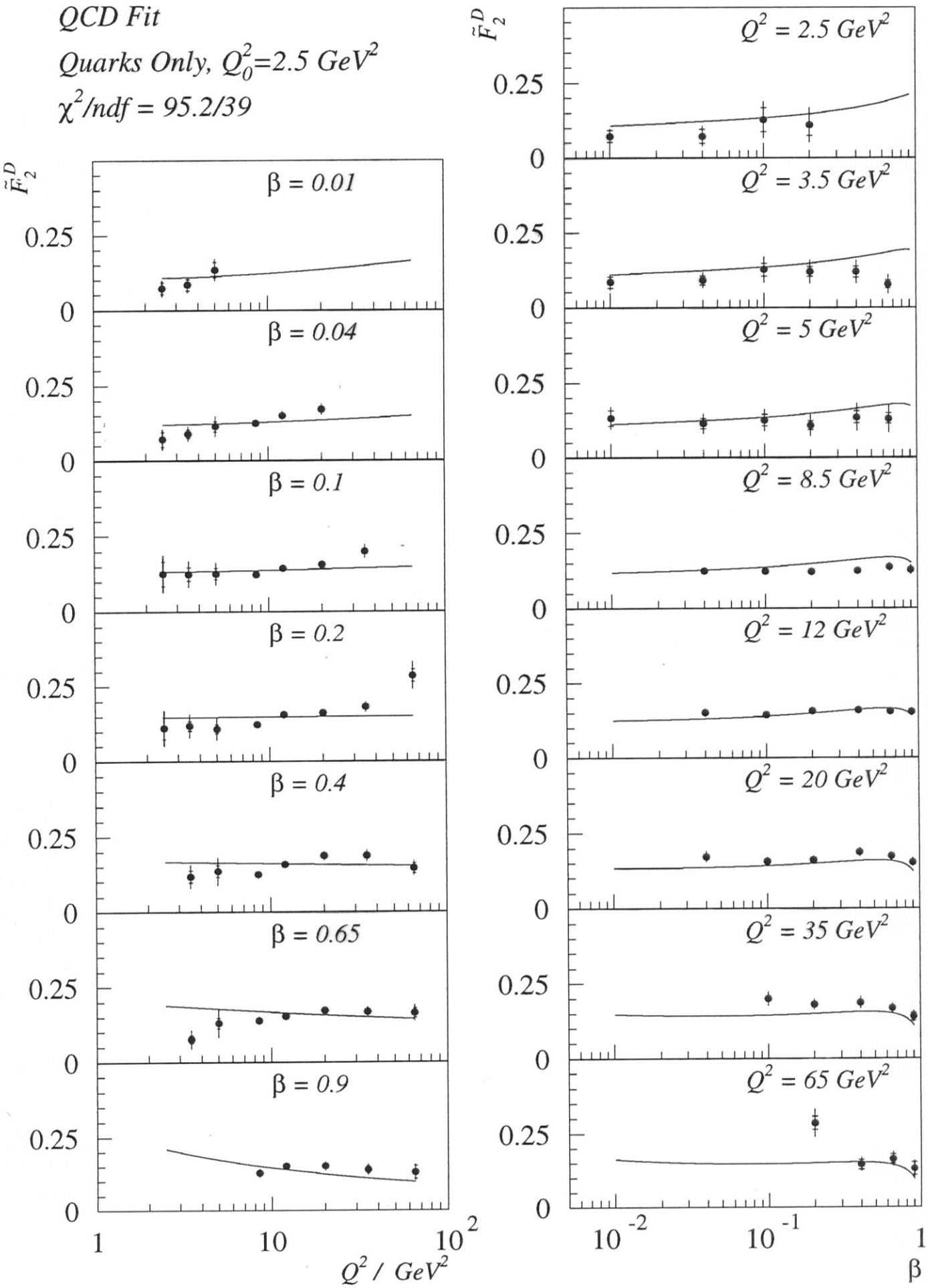

H1 Preliminary 1994

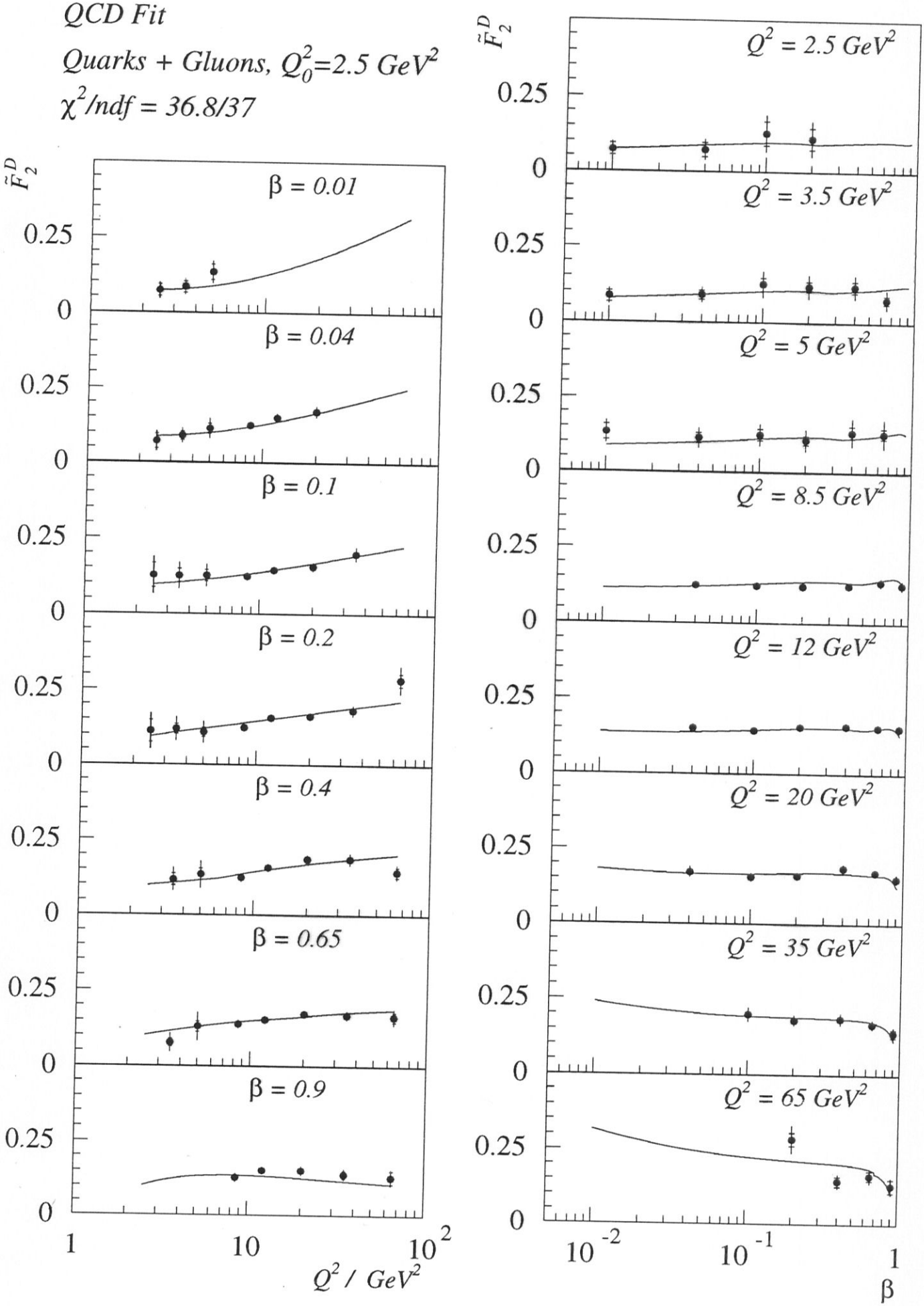

H1 Preliminary 1994

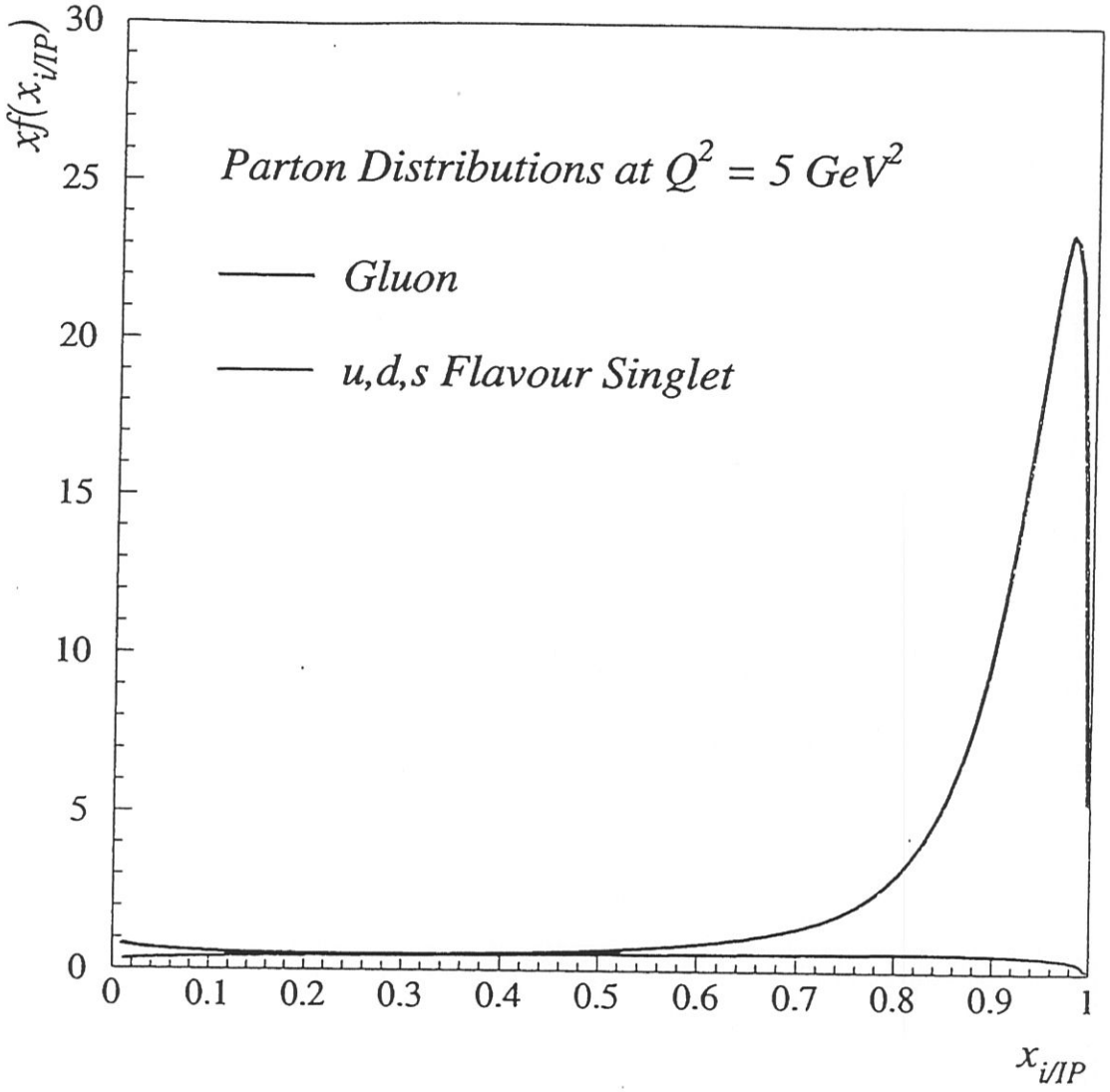

Normalisation set by fitting $\tilde{F}_2^D(\beta, Q^2)$ where

$$\tilde{F}_2^D(\beta, Q^2) = \int_{x_{I\!P}^L}^{x_{I\!P}^H} F_2^{D(3)}(\beta, Q^2, x_{I\!P})\, \mathrm{d}x_{I\!P}$$

($x_{I\!P}^L = 0.0003$ and $x_{I\!P}^H = 0.05$ as for 93 data)

Q^2 Evolution of Parton Densities

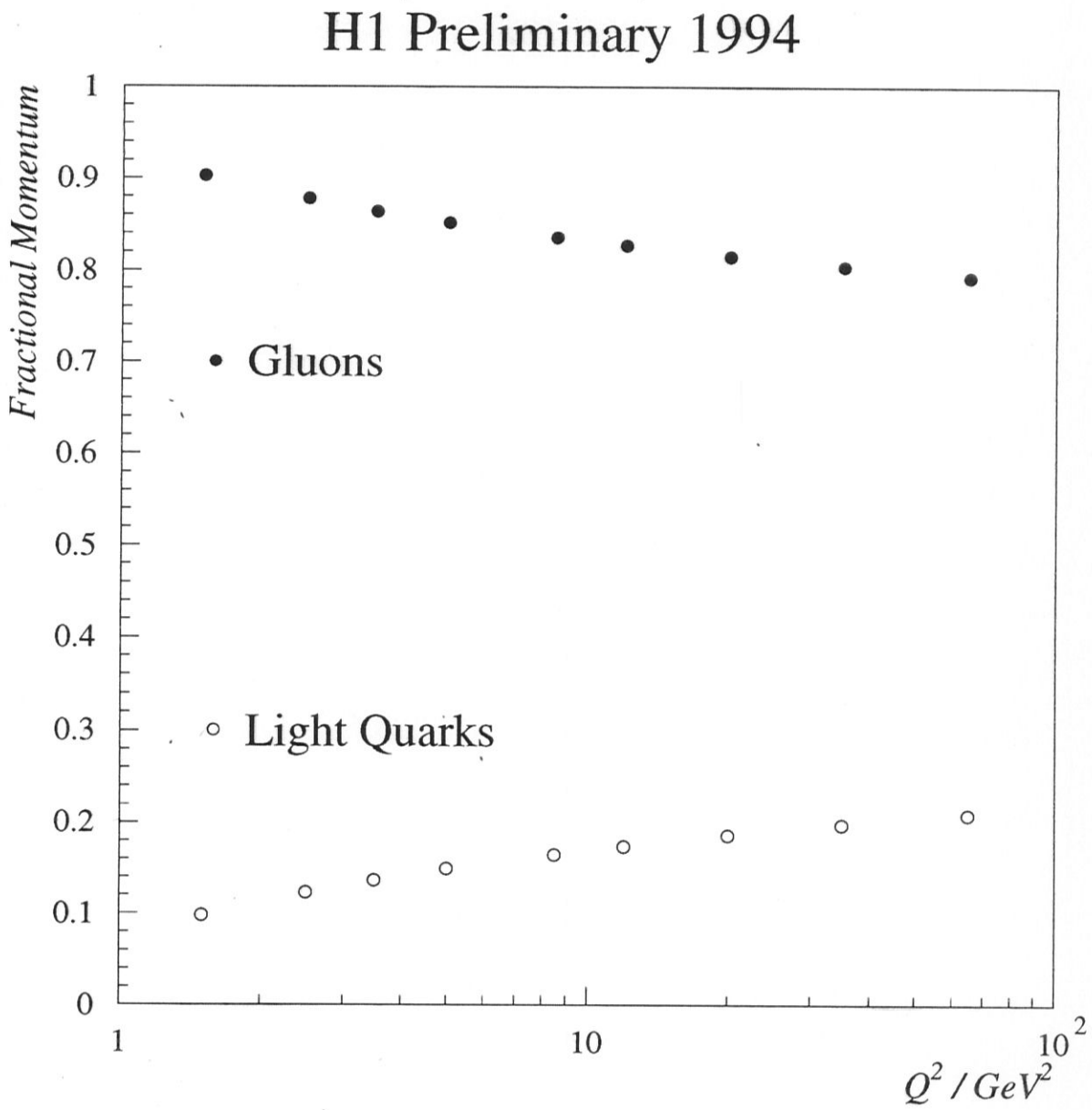

QCD Analysis of $\tilde{F}_2^D(\beta, Q^2)$

- Fit tends to singularity for gluon at $x_{i/I\!P} = 1$
- Parameterisation is restricted to avoid the singularity and ensure an accurate solution. ($B_g < 20$, $C_g > 0.1$) [$xg(x) \sim x^{B_g}(1-x)^{C_g}$]
- Better theoretical understanding of how to treat very high $x_{i/I\!P}$ region needed to proceed further
- The χ^2 is acceptable, and qualitatively, the picture is clear.
- Supporting evidence for interpretation as "leading gluon" phenomena (*cf* Buchmüller, Hebecker *et al*)

Conclusions for Deep-Inelastic Diffraction

- $F_2^{D(3)}(Q^2, \beta, x_{I\!P})$ has been measured over a wider kinematic range, and with higher precision than has previously been possible.
- Factorisation breaking as a function of β is observed.
- The origin of the factorisation breaking is not yet clear.
- $\tilde{F}_2^D(Q^2, \beta)$ displays clear scaling violations.
- $\tilde{F}_2^D(Q^2, \beta)$ is flat in β.
- There is evidence for a leading gluon structure to the diffractive exchange.